

Lagrangian approach and shape gradient for inverse problem of breaking line identification in solid: contact with adhesion

Victor A Kovtunenکو^{1,2} 

¹ Department of Mathematics and Scientific Computing, Karl-Franzens University of Graz, NAWI Graz, Heinrichstraße 36, Graz 8010, Austria

² Lavrentyev Institute of Hydrodynamics, Siberian Division of the Russian Academy of Sciences, 630090 Novosibirsk, Russia

E-mail: victor.kovtunenکو@uni-graz.at

Received 24 January 2023; revised 11 May 2023

Accepted for publication 16 June 2023

Published 28 June 2023



CrossMark

Abstract

A class of inverse identification problems constrained by variational inequalities is studied with respect to its shape differentiability. The specific problem appearing in failure analysis describes elastic bodies with a breaking line subject to simplified adhesive contact conditions between its faces. Based on the Lagrange multiplier approach and smooth Lavrentiev penalization, a semi-analytic formula for the shape gradient of the Lagrangian linearized on the solution is proved, which contains both primal and adjoint states. It is used for the descent direction in a gradient algorithm for identification of an optimal shape of the breaking line from boundary measurements. The theoretical result is supported by numerical simulation tests of destructive testing in 2D configuration with and without contact.

Keywords: shape optimal control, variational inequality, Lavrentiev penalization, free discontinuity problem, non-penetrating crack, adhesive contact, destructive testing.

(Some figures may appear in colour only in the online journal)



Original Content from this work may be used under the terms of the [Creative Commons Attribution 4.0 licence](https://creativecommons.org/licenses/by/4.0/). Any further distribution of this work must maintain attribution to the author(s) and the title of the work, journal citation and DOI.

1. Introduction

We prove rigorously the shape gradient for a class of inverse identification problems, which are constrained by penalty equations approximating variational inequalities (VIs). The specific problem describes identification of a breaking line in a body, where the fracture (crack) separating the single solid into two pieces allows adhesive contact.

The main drawback of classical hypotheses of brittle fracture mechanics according to Griffith [18] concerns infinite stresses in the vicinity of a crack which are physically inconsistent. Within a quasi-brittle fracture approach, there are several concepts that provide finite stresses by assuming a plastic zone around the crack tip, or taking into account inelastic phenomena at the crack faces being in contact. In [39] there is given a historical overview on modeling of non-ideal contact beginning from Coulomb's work on friction [10] up to the work of Johnson–Kendall–Roberts on adhesion of elastic bodies [26], validated with experiments. A comprehensive review of modern theories and experimental studies for adhesive joints and their failure can be found in [45]. Based on observations of hydraulic fracturing [46], Barenblatt underlied a cohesive crack model, which laid the foundation of the nonlinear fracture mechanics today. In opposite to the classical stress-free crack, in the work [3] he introduced two crucial hypotheses that crack faces close smoothly, and the normal stress is a function of the crack opening. Two representative functions $f(\delta)$ of the material dependence between the interaction force f and the crack opening δ according to Barenblatt's model and the bi-linear traction-separation law adopted in hydraulic fracturing are sketched in figure 1. A simplified model can be derived by applying the method of asymptotic expansion with respect to the thickness of interface adhesive layer, see e.g. [40], which asymptotic limit results in the spring model with linear $f = \alpha\delta$. The corresponding potential of the surface energy at the interface is quadratic with respect to opening. In this work we examine the case in relation to identifiability of the adhesive crack as a part of breaking line in a body.

Let Ω_t denote a set of geometric variables depending on a time-parameter t , which is determined by a manifold (the breaking line) Σ_t with a normal vector ν_t . Motivated by the applications in fracture, we consider a functional of the total energy $\mathcal{E}(u; \Omega_t)$ given over a Hilbert space $V(\Omega_t)$ as the sum of bulk and surface energies. The contact condition for the normal opening $\nu_t \cdot \llbracket u \rrbracket \geq 0$ across Σ_t (see [27]) determines the feasible set $K(\Omega_t) \subset V(\Omega_t)$, which topology implies a convex cone. For differentiable functions \mathcal{E} , minimization of $\mathcal{E}(u; \Omega_t)$ over $u \in K(\Omega_t)$ yields the first order optimality condition

$$u_t \in K(\Omega_t), \quad \langle \partial_u \mathcal{E}(u_t; \Omega_t), u - u_t \rangle \geq 0 \quad \text{for all } u \in K(\Omega_t). \quad (1.1)$$

The VI (1.1) constitutes the forward problem.

The variational formulation (1.1) was employed earlier [28, 30] for the description of non-penetrating cracks (implying that Σ_t has singularity at the crack tip), and supported by appropriate numerical methods [23, 29]. The surface energies were specified taking into account for adhesion [15] and cohesion [32, 41], where the latter results in non-smooth and non-convex functionals \mathcal{E} . For non-differentiable energies, see respective hemi-VI approaches in [19, 42]. We cite [43] for the concept of the conical differential of a solution to the Signorini VI. In [22] sensitivity estimates in shape optimization problems were investigated for a class of semi-linear elliptic VIs based on material derivatives. In [24] shape sensitivity analysis for an inverse obstacle problem and its regularization via penalization was performed by use of geometric properties of active and biactive sets.

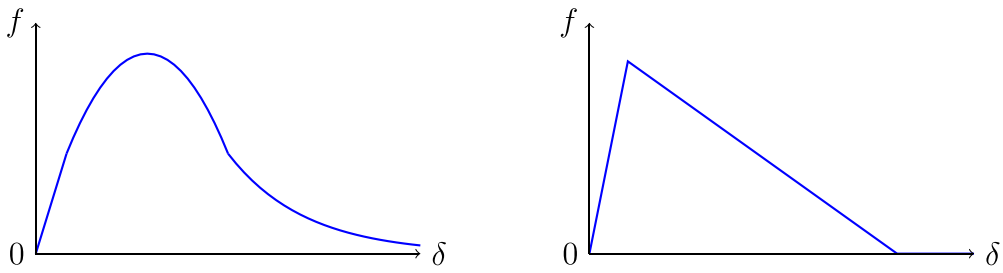


Figure 1. Sketch of dependence of interaction force f versus opening δ according to the models by Barenblatt (left) and hydro-fracking (right).

The inverse problem consists in identification of the manifold Σ_t from a measurement z given at an observation boundary Γ_t^O . Using the optimization formalism [25], we minimize the least-squares objective

$$\min \mathcal{J}(u_t; \Omega_t) = \frac{1}{2} \int_{\Gamma_t^O} |u_t - z|^2 dS_x + \rho |\Sigma_t|, \tag{1.2}$$

where u_t solves (1.1), and a parameter $\rho > 0$ implies the perimeter regularization. The VI (1.1) is involved in the optimization as an equilibrium constraint.

We cite the optimization-based inverse problems in acoustic scattering [1, 4], electrical tomography [8, 21], fluid mechanics [33], and free boundary problems [20]. The classical theory of inverse problems and its applications in mathematical physics can be found in [35]. For relevant tasks, see optimal control of partial differential equations (PDEs) [7], shape control of VIs [2], and optimal object location [36]. The shape optimization approach was applied for the inverse problem of identification of interfaces [14], geometric objects [31], inhomogeneities [6], and breaking lines [16].

Our main goal consists in deriving optimality conditions for the equilibrium constrained minimization (1.2) with respect to variations of the shape Σ_t . This implies a property of directional differentiability. To construct a differentiable approximation of the VI (1.1), for a regularization parameter $\varepsilon > 0$ and a smooth penalty β_ε based on the Lavrentiev regularization (see [38]):

$$\langle \partial_u^\varepsilon \mathcal{E}(u_t^\varepsilon; \Omega_t), u \rangle := \langle \partial_u \mathcal{E}(u_t^\varepsilon; \Omega_t), u \rangle + \int_{\Sigma_t} \beta_\varepsilon(\nu_t \cdot \llbracket u_t^\varepsilon \rrbracket) (\nu_t \cdot \llbracket u \rrbracket) dS_x \tag{1.3}$$

we introduce the penalized equilibrium equation: find $u_t^\varepsilon \in V(\Omega_t)$ such that

$$\langle \partial_u^\varepsilon \mathcal{E}(u_t^\varepsilon; \Omega_t), u \rangle = 0 \quad \text{for all } u \in V(\Omega_t). \tag{1.4}$$

However, the standard Lagrangian resulting from (1.2) and (1.4)

$$\mathcal{L}^\varepsilon(u, v; \Omega_t) := \mathcal{J}(u; \Omega_t) - \langle \partial_u^\varepsilon \mathcal{E}(u; \Omega_t), v \rangle \tag{1.5}$$

is conjectured to be not shape-differentiable. For this reason we compute a directional derivative with respect to specific shape perturbations, which give descent directions for the shape optimization problem. It coincides with the usual shape derivative in case of linear state equations.

The principal difficulty concerns non-linearity of the operator $\partial_u^\varepsilon \mathcal{E}$ due to the presence of penalty term in (1.3), even for linear $\partial_u \mathcal{E}$. Let the second variation $\partial_u(\partial_u^\varepsilon \mathcal{E})(u_t^\varepsilon; \Omega_t) \in$

$\mathcal{L}(V(\Omega_t), V(\Omega_t)^*)$ in (1.3) exist, be surjective with respect to u_t^ε , and the Lagrange identity hold at the solution:

$$\partial_u(\partial_u^\varepsilon \mathcal{E})(u_t^\varepsilon; \Omega_t)u_t^\varepsilon = \partial_u^\varepsilon \mathcal{E}(u_t^\varepsilon; \Omega_t) - \partial_u^\varepsilon \mathcal{E}(0; \Omega_t), \quad (1.6)$$

where $V(\Omega_t)^*$ denotes the dual space. Then the associated adjoint operator $[\partial_u(\partial_u^\varepsilon \mathcal{E})(u_t^\varepsilon; \Omega_t)]^* \in \mathcal{L}(V(\Omega_t), V(\Omega_t)^*)$ can be well-defined by the formula

$$\langle [\partial_u(\partial_u^\varepsilon \mathcal{E})(u_t^\varepsilon; \Omega_t)]^* v, u \rangle := \langle \partial_u(\partial_u^\varepsilon \mathcal{E})(u_t^\varepsilon; \Omega_t)u, v \rangle \quad \text{for } u, v \in V(\Omega_t), \quad (1.7)$$

see [5, 34, 37]. We set a corresponding Lagrangian linearized at the solution u_t^ε as

$$\tilde{\mathcal{L}}^\varepsilon(0, u_t^\varepsilon, u, v; \Omega_t) := \mathcal{J}(u; \Omega_t) - \langle [\partial_u(\partial_u^\varepsilon \mathcal{E})(u_t^\varepsilon; \Omega_t)]^* v, u \rangle - \langle \partial_u^\varepsilon \mathcal{E}(0; \Omega_t), v \rangle \quad (1.8)$$

which coincides with $\mathcal{L}^\varepsilon(u, v; \Omega_t)$ in (1.5) as $u = u_t^\varepsilon$ in virtue of (1.6).

Now we formulate the saddle-point problem: find $(u_t^\varepsilon, v_t^\varepsilon) \in V(\Omega_t)^2$ such that

$$\tilde{\mathcal{L}}^\varepsilon(0, u_t^\varepsilon, u_t^\varepsilon, v; \Omega_t) \leq \tilde{\mathcal{L}}^\varepsilon(0, u_t^\varepsilon, u_t^\varepsilon, v_t^\varepsilon; \Omega_t) \leq \tilde{\mathcal{L}}^\varepsilon(0, u_t^\varepsilon, u, v_t^\varepsilon; \Omega_t) \quad (1.9)$$

for all $(u, v) \in V(\Omega_t)^2$. The primal inf-sup condition (the former inequality in (1.9)) follows the equilibrium problem (1.4). The dual sup-inf condition implies the latter inequality in (1.9) (see [12, chapter 6]). For differentiable objectives \mathcal{J} it leads to the adjoint equation: for fixed $u_t^\varepsilon \in V(\Omega_t)$, find $v_t^\varepsilon \in V(\Omega_t)$ such that

$$\langle \partial_u \mathcal{J}(u_t^\varepsilon; \Omega_t) - [\partial_u(\partial_u^\varepsilon \mathcal{E})(u_t^\varepsilon; \Omega_t)]^* v_t^\varepsilon, v \rangle = 0 \quad \text{for all } v \in V(\Omega_t). \quad (1.10)$$

Based on the concept of directional differentiability [9, 11] we look for a shape gradient of the objective linked to the Lagrangian:

$$\partial_t \mathcal{J}(u_t^\varepsilon; \Omega_t) = \partial_t \tilde{\mathcal{L}}^\varepsilon(0, u_t^\varepsilon, u_t^\varepsilon, v_t^\varepsilon; \Omega_t) \quad (1.11)$$

since the identity $\mathcal{J}(u_t^\varepsilon; \Omega_t) = \tilde{\mathcal{L}}^\varepsilon(0, u_t^\varepsilon, u_t^\varepsilon, v_t^\varepsilon; \Omega_t)$ is attained in (1.8) at the saddle point. Then negative sign $\partial_t \mathcal{J}(u_t^\varepsilon; \Omega_t) < 0$ provides a descent direction for minimization (1.2). Using a Hadamard representation of the shape gradient at Σ_t , which is performed with the help of the saddle point $(u_t^\varepsilon, v_t^\varepsilon)$ and kinematic velocity Λ as

$$\partial_t \mathcal{J}(u_t^\varepsilon; \Omega_t) = \int_{\Sigma_t} \Lambda \cdot \mathcal{D}(u_t^\varepsilon, u_t^\varepsilon) dS_x, \quad (1.12)$$

the negative sign is achieved by the choice $\Lambda = -k\mathcal{D}(u_t^\varepsilon, u_t^\varepsilon)$ with a free factor $k > 0$. Then an iterative algorithm can be constructed, which subsequently updates the current manifold Σ_t by $\Sigma_t + \Lambda$.

Recently, the shape gradient in (1.6)–(1.12) was obtained for semi-linear equilibrium equations due to the turbulent flow [17] and cohesive contact [32] phenomena. In the present work we apply the shape optimization algorithm to inverse problems identifying a breaking-line subject to adhesive contact and examine it by numerical simulation.

2. Solid with a breaking-line subject to contact with adhesion

Let $\Omega \subset \mathbb{R}^d$, where dimensions $d = 2$ or $d = 3$ are physically relevant, be a hold-all domain with Lipschitz boundary $\partial\Omega$ and normal vector $n_t = ((n_t)_1, \dots, (n_t)_d)$ outward to Ω . The domain $\Omega = \Omega_t^+ \cup \Omega_t^- \cup \Sigma_t$ is assumed being broken by a manifold Σ_t into two variable sub-domains Ω_t^\pm depending on the time-parameter $t \in (t_0, t_1)$, $t_0 < t_1$. It has Lipschitz boundaries $\partial\Omega_t^\pm$ with outward normal vectors n_t^\pm coinciding with n_t at $\partial\Omega$, and $n_t^- = -n_t^+ =: \nu_t$ at the breaking line $\Sigma_t = \partial\Omega_t^+ \cap \partial\Omega_t^-$. By this, the outer boundary is split into two variable parts $\partial\Omega = \overline{\Gamma_t^D} \cup \overline{\Gamma_t^N}$, and $\Gamma_t^D \cap \Gamma_t^N = \emptyset$. The conditions $\Gamma_t^D \cap \partial\Omega_t^+ \neq \emptyset$ and $\Gamma_t^D \cap \partial\Omega_t^- \neq \emptyset$ are required for the

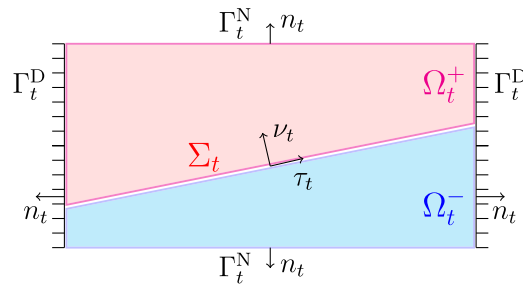


Figure 2. An example configuration of the variable geometry Ω_t in 2D.

Korn–Poincaré inequality (2.4). Let an observation boundary $\Gamma_t^O \subset \Gamma_t^N$. We assume that these geometric properties are preserved for all $t \in (t_0, t_1)$ under shape perturbations specified below.

We define a parameter-dependent set of geometric objects $\Omega_t = (\Gamma_t^D, \Gamma_t^N, \Gamma_t^O, \Sigma_t)$ describing the broken domain $\Omega \setminus \Sigma_t = \Omega_t^+ \cup \Omega_t^-$, which includes the Dirichlet, Neumann, observation boundaries, and the breaking line (manifold in 3D), respectively. An example geometry of Ω_t is sketched in figure 2 in 2D.

For fixed t , we consider a linear elastic body occupying the broken domain $\Omega \setminus \Sigma_t$. The displacement vector $u(x) = (u_1, \dots, u_d)$ at points $x = (x_1, \dots, x_d)$ has discontinuity across Σ_t with the jump $[[u]] = u|_{\Sigma_t \cap \partial\Omega_t^+} - u|_{\Sigma_t \cap \partial\Omega_t^-}$. We decompose $[[u]]$ at the interface into the normal component $\nu_t \cdot [[u]]$ and the tangential vector $[[u]]_{\tau_t}$ such that

$$[[u]] = (\nu_t \cdot [[u]])\nu_t + [[u]]_{\tau_t}, \quad \nu_t \cdot [[u]] \geq 0 \quad \text{on } \Sigma_t, \tag{2.1}$$

where the latter inequality guarantees non-penetration, see [27]. Using (2.1) we prescribe adhesion at Σ_t with the help of quadratic surface energy (see [15, 42]):

$$\mathcal{S}([[u]]; \Sigma_t) = \frac{\alpha}{2} \int_{\Sigma_t} \{ |[[u]]_{\tau_t} |^2 + (\nu_t \cdot [[u]]) ^2 \} dS_x, \quad \alpha \geq 0. \tag{2.2}$$

The symmetric tensors of linearized strain $\epsilon = (\epsilon_{ij})_{i,j=1}^d$ and Cauchy stress $\sigma = (\sigma_{ij})_{i,j=1}^d$ are given by the symmetric gradient and Hooke’s law:

$$\epsilon(u) = \frac{1}{2}(\nabla u + \nabla u^\top), \quad \sigma(u) = C\epsilon(u), \tag{2.3}$$

where the gradient $\nabla u = (\partial u_i / \partial x_j)_{i,j=1}^d$, the transposition $^\top$ swaps columns for rows. A fourth order tensor of elastic coefficients $C(x) \in W^{1,\infty}(\Omega)^{d \times d \times d \times d}$ is symmetric: $C_{ijkl} = C_{jikl} = C_{klij}$ for $i, j, k, l = 1, \dots, d$, and positive definite. The scalar product of tensors in (2.3) satisfies the Korn–Poincaré inequality: there exists $K_{KP} > 0$ such that

$$\int_{\Omega \setminus \Sigma_t} \sigma(u) \cdot \epsilon(u) dx \geq K_{KP} \|u\|_{H^1(\Omega \setminus \Sigma_t)}^2 \quad \text{for } u \in V(\Omega_t) \tag{2.4}$$

over the Sobolev space accounting for the Dirichlet boundary condition:

$$V(\Omega_t) = \{u \in H^1(\Omega_t^+) \cap H^1(\Omega_t^-) \mid u = 0 \text{ on } \Gamma_t^D\}. \tag{2.5}$$

For a boundary force $g = (g_1, \dots, g_d) \in H^1(\partial\Omega)^d$, we introduce the bulk energy

$$\mathcal{B}(u; \Omega_t) = \frac{1}{2} \int_{\Omega \setminus \Sigma_t} \sigma(u) \cdot \epsilon(u) dx - \int_{\Gamma_t^N} g \cdot u dS_x. \tag{2.6}$$

The feasible set corresponding to the constraint in (2.1) due to contact reads

$$K(\Omega_t) = \{u \in V(\Omega_t) \mid \nu_t \cdot \llbracket u \rrbracket \geq 0 \text{ on } \Sigma_t\}, \quad (2.7)$$

and its topology implies a convex and closed cone.

Theorem 1 (Solvability of the adhesive contact problem). *There exists a unique solution $u_t \in K(\Omega_t)$ to the constrained minimization problem:*

$$\mathcal{E}(u_t; \Omega_t) = \min_{u \in K(\Omega_t)} \mathcal{E}(u; \Omega_t) := \mathcal{B}(u; \Omega_t) + \mathcal{S}(\llbracket u \rrbracket; \Sigma_t), \quad (2.8)$$

where the total energy \mathcal{E} is composed according to (2.2) and (2.6) as the sum

$$\mathcal{E}(u; \Omega_t) = \frac{1}{2} \int_{\Omega \setminus \Sigma_t} \sigma(u) \cdot \epsilon(u) dx - \int_{\Gamma_t^N} g \cdot u dS_x + \frac{\alpha}{2} \int_{\Sigma_t} |\llbracket u \rrbracket|^2 dS_x. \quad (2.9)$$

The solution satisfies a first-order optimality condition in the form of VI:

$$\begin{aligned} & \langle \partial_u \mathcal{E}(u_t; \Omega_t), u - u_t \rangle \\ & := \int_{\Omega \setminus \Sigma_t} \sigma(u_t) \cdot \epsilon(u - u_t) dx + \alpha \int_{\Sigma_t} \{ \llbracket u_t \rrbracket_{\tau_t} \cdot \llbracket u - u_t \rrbracket_{\tau_t} \\ & \quad + (\nu_t \cdot \llbracket u_t \rrbracket) (\nu_t \cdot \llbracket u - u_t \rrbracket) \} dS_x - \int_{\Gamma_t^N} g \cdot (u - u_t) dS_x \geq 0 \end{aligned} \quad (2.10)$$

for all $u \in K(\Omega_t)$. The H^2 -smooth solution satisfies the boundary value problem:

$$\operatorname{div} \sigma(u_t) = 0 \quad \text{in } \Omega \setminus \Sigma_t, \quad (2.11a)$$

$$u_t = 0 \quad \text{on } \Gamma_t^D, \quad (2.11b)$$

$$\sigma(u_t)n = g \quad \text{on } \Gamma_t^N, \quad (2.11c)$$

$$\llbracket \sigma(u_t) \nu_t \rrbracket = 0 \quad \text{on } \Sigma_t, \quad (2.11d)$$

$$(\sigma(u_t) \nu_t)_{\tau_t} = \alpha \llbracket u_t \rrbracket_{\tau_t} \quad \text{on } \Sigma_t, \quad (2.11e)$$

$$\begin{aligned} & \nu_t \cdot \llbracket u_t \rrbracket \geq 0, \quad \nu_t \cdot (\sigma(u_t) \nu_t) \leq \alpha (\nu_t \cdot \llbracket u_t \rrbracket), \\ & (\nu_t \cdot \llbracket u_t \rrbracket) \{ \nu_t \cdot (\sigma(u_t) \nu_t) - \alpha (\nu_t \cdot \llbracket u_t \rrbracket) \} = 0 \quad \text{on } \Sigma_t \end{aligned} \quad (2.11f)$$

decomposing the normal stress $\sigma(u_t) \nu_t = (\nu_t \cdot (\sigma(u_t) \nu_t)) \nu_t + (\sigma(u_t) \nu_t)_{\tau_t}$ according to (2.1).

Proof. Indeed, applying standard variational arguments to the quadratic functional in (2.9) implies the VI (2.10). Its operator $\partial_u \mathcal{E}$ builds a continuous bilinear form in $V(\Omega_t)^2$, which is coercive by the virtue of Korn–Poincaré inequality (2.4). Then a unique minimizer is argued by the Lions–Stampacchia theorem.

For the derivation of boundary-value problem (2.11a)–(2.11f), see the variational theory and method treating non-penetration conditions in [27, section 1.4]. The relations (2.11a) describe equilibrium, (2.11b)—clamping, (2.11c)—boundary traction, (2.11d)—continuity of stress, (2.11e)—tangential stress, and two lines in (2.11f) are the complementarity conditions for the normal stress due to contact. \square

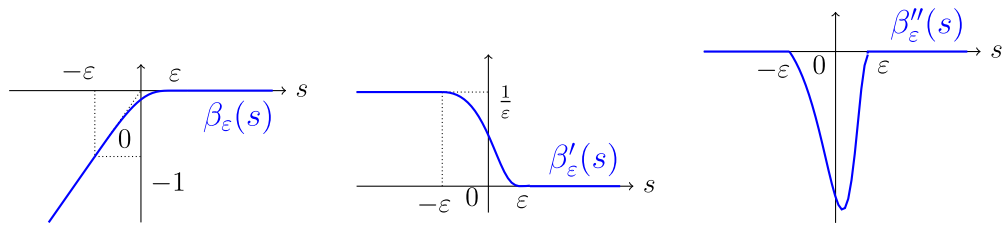


Figure 3. Lavrentiev penalty function β_ε , its derivatives β'_ε and β''_ε .

For the penalty parameter $\varepsilon \in (0, \varepsilon_0)$, $\varepsilon_0 > 0$, we approximate the VI (2.10) using smooth Lavrentiev penalization. For example, let a C^1 -smooth penalty function $\beta_\varepsilon(s)$ be given by mollification of the standard penalty $\min(0, s)/\varepsilon$ as

$$\beta_\varepsilon(s) = \begin{cases} s/\varepsilon & \text{for } s < -\varepsilon \\ -\exp(2(s + \varepsilon)/(s - \varepsilon)) & \text{for } -\varepsilon \leq s < \varepsilon \\ 0 & \text{for } s \geq \varepsilon \end{cases} \quad (2.12)$$

which is depicted in figure 3 together with the first and second derivatives.

Lemma 1 (Properties of the penalty). *The penalty function in (2.12) $\beta_\varepsilon \leq 0$ is concave and increases monotonically, the derivative $\beta'_\varepsilon \geq 0$ and decreases monotonically, the second derivative $\beta''_\varepsilon \leq 0$. It satisfies the following uniform estimates*

$$-1 \leq \beta_\varepsilon(s) - \frac{\min(0, s)}{\varepsilon} \leq 0, \quad 0 \leq \beta'_\varepsilon(s) \leq \frac{1}{\varepsilon}, \quad (2.13)$$

the relaxed complementarity and compliance conditions, respectively:

$$\beta_\varepsilon(s) \max(0, s) \geq -\varepsilon, \quad -\beta_\varepsilon(s) \min(0, s) \leq -\frac{\min^2(0, s)}{\varepsilon}. \quad (2.14)$$

Proof. The properties (2.13) can be checked straightforwardly.

To verify the former inequality in (2.14), multiplying (2.12) by $\max(0, s)$ we deduce that $\beta_\varepsilon(s) \max(0, s) = 0$ for $s \geq \varepsilon$. Using $\beta_\varepsilon(s) \geq \min(0, s)/\varepsilon - 1$ from the first estimate in (2.13), the lower bound $\beta_\varepsilon(s) \max(0, s) \geq -\varepsilon$ holds for $0 \leq s < \varepsilon$.

By the similar arguments, $-\beta_\varepsilon(s) \min(0, s) = -\min^2(0, s)/\varepsilon$ for $s < -\varepsilon$ and $s \geq 0$ in (2.12). The second estimate $\beta_\varepsilon(s) \leq \min(0, s)/\varepsilon$ in (2.13), after multiplication with $-\min(0, s)$ leads to the upper bound $-\beta_\varepsilon(s) \min(0, s) \leq -\min^2(0, s)/\varepsilon$ for $-\varepsilon \leq s < 0$. This proves the latter inequality in (2.14). \square

From lemma 1 we deduce solvability for the ε -penalized problem.

Theorem 2 (Solvability of the Lavrentiev penalization). *There exists a unique solution $u_t^\varepsilon \in V(\Omega_t)$ to the penalty problem:*

$$\begin{aligned} \langle \partial_u^\varepsilon \mathcal{E}(u_t^\varepsilon; \Omega_t), u \rangle := & \int_{\Omega \setminus \Sigma_t} \sigma(u_t^\varepsilon) \cdot \epsilon(u) \, dx + \int_{\Sigma_t} \{ \alpha [[u_t^\varepsilon]]_{\tau_t} \cdot [[u]]_{\tau_t} \\ & + [\alpha \text{id} + \beta_\varepsilon](\nu_t \cdot [[u_t^\varepsilon]]) (\nu_t \cdot [[u]]) \} \, dS_x - \int_{\Gamma_t^N} g \cdot u \, dS_x = 0 \end{aligned} \quad (2.15)$$

for all $u \in V(\Omega_t)$, where the identity transformation $id(s) = s$. The H^2 -smooth solution satisfies the following boundary value problem:

$$\operatorname{div} \sigma(u_t^\varepsilon) = 0 \quad \text{in } \Omega \setminus \Sigma_t, \quad (2.16a)$$

$$u_t^\varepsilon = 0 \quad \text{on } \Gamma_t^D, \quad (2.16b)$$

$$\sigma(u_t^\varepsilon)n = g \quad \text{on } \Gamma_t^N, \quad (2.16c)$$

$$[[\sigma(u_t^\varepsilon)\nu_t]] = 0 \quad \text{on } \Sigma_t, \quad (2.16d)$$

$$(\sigma(u_t^\varepsilon)\nu_t)_\tau = \alpha[[u_t^\varepsilon]]_\tau, \quad \text{on } \Sigma_t, \quad (2.16e)$$

$$\nu_t \cdot (\sigma(u_t^\varepsilon)\nu_t) = \alpha(\nu_t \cdot [[u_t^\varepsilon]]) + \beta_\varepsilon(\nu_t \cdot [[u_t^\varepsilon]]) \quad \text{on } \Sigma_t. \quad (2.16f)$$

Proof. Since $s = \max(0, s) + \min(0, s)$, inequalities (2.14) give $\beta_\varepsilon(s)s \geq (\min(0, s))^2/\varepsilon - \varepsilon$. Using the Cauchy–Schwarz, Korn–Poincaré (2.4), and the trace inequality

$$\|u\|_{L^2(\partial\Omega_t^\pm)^d} \leq \|u\|_{H^1/2(\partial\Omega_t^\pm)^d} \leq K_{\text{tr}}\|u\|_{H^1(\Omega_t^\pm)^d} \quad \text{for } u \in H^1(\Omega_t^\pm)^d \quad (2.17)$$

such that $\|[[u]]\|_{L^2(\Sigma_t)^d} \leq \sqrt{2}K_{\text{tr}}\|u\|_{H^1(\Omega_t^\pm)^d}$, the operator in (2.15) satisfies

$$\begin{aligned} \langle \partial_u^\varepsilon \mathcal{E}(u_t^\varepsilon; \Omega_t), u_t^\varepsilon \rangle &\geq K_{\text{KP}}\|u_t^\varepsilon\|_{H^1(\Omega \setminus \Sigma_t)^d}^2 + \alpha\|[[u_t^\varepsilon]]\|_{L^2(\Sigma_t)^d}^2 \\ &\quad - K_{\text{tr}}(\varepsilon\sqrt{2|\Sigma_t|} + \|g\|_{L^2(\Gamma_t^N)^d})\|u_t^\varepsilon\|_{H^1(\Omega \setminus \Sigma_t)^d}, \end{aligned} \quad (2.18)$$

thus, it is coercive. The penalty β_ε is uniformly continuous preserving L^2 -convergence, then operator $\partial_u^\varepsilon \mathcal{E}$ is weakly continuous: if $u^n \rightharpoonup u_t$ weakly in $H^1(\Omega \setminus \Sigma_t)^d$ as $n \rightarrow \infty$ (hence $u^n \rightarrow u_t$ strongly in $L^2(\partial\Omega \cup \Sigma_t^\pm)^d$ by compactness), then $\langle \partial_u^\varepsilon \mathcal{E}(u^n; \Omega_t), u \rangle \rightarrow \langle \partial_u^\varepsilon \mathcal{E}(u_t; \Omega_t), u \rangle$ for $u \in V(\Omega_t)$. Therefore, applying a Galerkin approximation and the Brouwer fixed point theorem (see [13]) justifies a solution to the variational problem (2.15). The uniqueness due to the strict monotony, and the boundary value formulation (2.16a)–(2.16f) can be derived in a standard way. \square

Next we consider the inverse identification problem.

3. Inverse problem and shape gradient for the linearized Lagrangian

For a given observation $z \in H^1(\partial\Omega)^d$, we consider the least-squares objective in (1.2):

$$\mathcal{J}(u_t^\varepsilon; \Omega_t) = \frac{1}{2} \int_{\Gamma_t^o} |u_t^\varepsilon - z|^2 dS_x + \rho|\Sigma_t|, \quad (3.1)$$

where u_t^ε solves the penalty equation (2.15). From the fundamental theorem of calculus, the following representation holds for continuous β'_ε :

$$\beta_\varepsilon(\nu_t \cdot [[u_t^\varepsilon]]) = \int_0^1 \beta'_\varepsilon(\nu_t \cdot [ru_t^\varepsilon]) (\nu_t \cdot [[u_t^\varepsilon]]) dr + \beta_\varepsilon(0). \quad (3.2)$$

We introduce a quadratic Lagrangian linearized according to (3.2) around the solution u_t^ε to penalty equation (2.15) as follows (see [32]):

$$\begin{aligned} \tilde{\mathcal{L}}^\varepsilon(0, u_t^\varepsilon, u, v; \Omega_t) := & \frac{1}{2} \int_{\Gamma_t^0} |u - z|^2 dS_x + \rho |\Sigma_t| \\ & - \int_{\Omega \setminus \Sigma_t} \sigma(u) \cdot \epsilon(v) dx + \int_{\Gamma_t^N} g \cdot v dS_x - \int_{\Sigma_t} \left\{ \alpha \llbracket u \rrbracket_{\tau_t} \cdot \llbracket v \rrbracket_{\tau_t} \right. \\ & \left. + \left[\alpha \nu_t \cdot \llbracket u \rrbracket + \int_0^1 \beta'_\varepsilon(\nu_t \cdot \llbracket ru_t^\varepsilon \rrbracket) (\nu_t \cdot \llbracket u \rrbracket) dr + \beta_\varepsilon(0) \right] (\nu_t \cdot \llbracket v \rrbracket) \right\} dS_x \end{aligned} \quad (3.3)$$

The corresponding saddle point problem reads: find $(u_t^\varepsilon, v_t^\varepsilon) \in V(\Omega_t)^2$ such that

$$\tilde{\mathcal{L}}^\varepsilon(0, u_t^\varepsilon, u_t^\varepsilon, v; \Omega_t) \leq \tilde{\mathcal{L}}^\varepsilon(0, u_t^\varepsilon, u_t^\varepsilon, v_t^\varepsilon; \Omega_t) \leq \tilde{\mathcal{L}}^\varepsilon(0, u_t^\varepsilon, u, v_t^\varepsilon; \Omega_t) \quad (3.4)$$

for all $(u, v) \in V(\Omega_t)^2$. According to (3.2) the optimal value of $\tilde{\mathcal{L}}^\varepsilon$ at the saddle point

$$\begin{aligned} \tilde{\mathcal{L}}^\varepsilon(0, u_t^\varepsilon, u_t^\varepsilon, v_t^\varepsilon; \Omega_t) = & \frac{1}{2} \int_{\Gamma_t^0} |u_t^\varepsilon - z|^2 dS_x + \rho |\Sigma_t| - \int_{\Omega \setminus \Sigma_t} \sigma(u_t^\varepsilon) \cdot \epsilon(v_t^\varepsilon) dx \\ & - \int_{\Sigma_t} \left\{ \alpha \llbracket u_t^\varepsilon \rrbracket_{\tau_t} \cdot \llbracket u_t^\varepsilon \rrbracket_{\tau_t} + [\alpha \text{id} + \beta_\varepsilon] (\nu_t \cdot \llbracket u_t^\varepsilon \rrbracket) (\nu_t \cdot \llbracket u_t^\varepsilon \rrbracket) \right\} dS_x \\ & + \int_{\Gamma_t^N} g \cdot v_t^\varepsilon dS_x \end{aligned}$$

due to (2.15) coincides with the objective (3.1):

$$\tilde{\mathcal{L}}^\varepsilon(0, u_t^\varepsilon, u_t^\varepsilon, v_t^\varepsilon; \Omega_t) = \mathcal{J}(u_t^\varepsilon; \Omega_t). \quad (3.5)$$

Theorem 3 (Solvability of the saddle-point problem). *There exists the unique saddle-point $(u_t^\varepsilon, v_t^\varepsilon) \in V(\Omega_t)^2$ in (3.4), which primal component u_t^ε solves (2.15). The dual component v_t^ε is a solution to the adjoint equation:*

$$\begin{aligned} \langle A_\varepsilon(u_t^\varepsilon, v_t^\varepsilon) \rangle := & \int_{\Omega \setminus \Sigma_t} \sigma(v) \cdot \epsilon(v_t^\varepsilon) dx + \int_{\Sigma_t} \left\{ \alpha \llbracket v \rrbracket_{\tau_t} \cdot \llbracket v_t^\varepsilon \rrbracket_{\tau_t} + \left[\alpha \nu_t \cdot \llbracket v \rrbracket \right. \right. \\ & \left. \left. + \int_0^1 \beta'_\varepsilon(\nu_t \cdot \llbracket ru_t^\varepsilon \rrbracket) (\nu_t \cdot \llbracket v \rrbracket) dr \right] (\nu_t \cdot \llbracket v_t^\varepsilon \rrbracket) \right\} dS_x = \int_{\Gamma_t^0} v \cdot (u_t^\varepsilon - z) dS_x \end{aligned} \quad (3.6)$$

for all $v \in V(\Omega_t)$. The H^2 -smooth solution satisfies the boundary value problem:

$$\text{div } \sigma(v_t^\varepsilon) = 0 \quad \text{in } \Omega \setminus \Sigma_t, \quad (3.7a)$$

$$v_t^\varepsilon = 0 \quad \text{on } \Gamma_t^D, \quad (3.7b)$$

$$\sigma(v_t^\varepsilon)n = 0 \quad \text{on } \Gamma_t^N \setminus \Gamma_t^O, \quad (3.7c)$$

$$\sigma(v_t^\varepsilon)n = u_t^\varepsilon - z \quad \text{on } \Gamma_t^O, \quad (3.7d)$$

$$\llbracket \sigma(v_t^\varepsilon) \nu_t \rrbracket = 0 \quad \text{on } \Sigma_t, \quad (3.7e)$$

$$(\sigma(v_t^\varepsilon) \nu_t)_\tau = \alpha \llbracket v_t^\varepsilon \rrbracket_\tau \quad \text{on } \Sigma_t, \quad (3.7f)$$

$$\nu_t \cdot (\sigma(v_t^\varepsilon) \nu_t) = \alpha \nu_t \cdot \llbracket v_t^\varepsilon \rrbracket + \int_0^1 \beta'_\varepsilon(\nu_t \cdot \llbracket ru_t^\varepsilon \rrbracket) (\nu_t \cdot \llbracket v_t^\varepsilon \rrbracket) dr \quad \text{on } \Sigma_t. \quad (3.7g)$$

Proof. The Lagrangian function $\tilde{\mathcal{L}}^\varepsilon$ from (3.3) is quadratic and convex in u , and linear in v . Therefore, the first order optimality condition for the former inequality in (3.4) is expressed using (3.2) by the primal variational equation (2.15), and by the adjoint variational equation (3.6) for the latter inequality in (3.4). The unique solution u_t^ε to (2.15) was proven in

theorem 2. For fixed u_t^ε , the bilinear form $A_\varepsilon(u_t^\varepsilon)$ in the left-hand side of (3.6) is bounded and coercive by virtue of the Korn–Poincaré inequality (2.4) and $\beta'_\varepsilon \geq 0$ in lemma 1, hence (3.6) has a unique solution by the Lax–Milgram theorem. The boundary value formulation (3.7a)–(3.7g) follows straightforwardly. \square

Next, the saddle-point problem (3.4) is perturbed by the velocity method [44]. We introduce the coordinate transformation $y = \phi_s(x)$ and its inverse $x = \phi_s^{-1}(y)$, where

$$\phi_s, \phi_s^{-1} \in C^1([t_0 - t_1, t_1 - t_0]; W^{1,\infty}(\bar{\Omega}))^d. \tag{3.8}$$

For fixed $t \in (t_0, t_1)$ and variable $s \in I := [t_0, t_1] - t$, we suppose a diffeomorphism

$$\phi_s : \Omega_t \mapsto \Omega_{t+s}, \quad x \mapsto y, \quad \phi_s^{-1} : \Omega_{t+s} \mapsto \Omega_t, \quad y \mapsto x, \tag{3.9}$$

which transforms the broken domain $\Omega \setminus \Sigma_t$ to $\Omega \setminus \Sigma_{t+s}$ by means of a perturbed geometry $\Omega_{t+s} = (\Gamma_{t+s}^D, \Gamma_{t+s}^N, \Gamma_{t+s}^O, \Sigma_{t+s})$. A kinematic velocity can be determined from (3.8) in the implicit way as

$$\Lambda(t+s, y) := \frac{d}{ds} \phi_s(\phi_s^{-1}(y)). \tag{3.10}$$

Conversely, let the kinematic velocity be given explicitly

$$\Lambda = (\Lambda_1, \dots, \Lambda_d)(t, x) \in C([t_0, t_1]; W^{1,\infty}(\bar{\Omega}))^d \tag{3.11}$$

preserving the hold-all domain Ω under the condition $n \cdot \Lambda = 0$ on $\partial\Omega$. It determines the flows (3.8) as solutions $\phi_s = ((\phi_s)_1, \dots, (\phi_s)_d)$ to the non-autonomous ODE system

$$\frac{d}{ds} \phi_s = \Lambda(t+s, \phi_s) \text{ for } s \in I, \quad \phi_s = x \text{ at } s = 0, \tag{3.12}$$

and $\phi_s^{-1}(y) = ((\phi_s^{-1})_1, \dots, (\phi_s^{-1})_d)$ to the transport equation

$$\frac{\partial}{\partial s} \phi_s^{-1} + (\nabla_y \phi_s^{-1}) \Lambda|_{t+s} = 0 \text{ in } I \times \Omega, \quad \phi_s^{-1} = y \text{ at } s = 0, \tag{3.13}$$

see [30], where the notation $\Lambda|_{t+s} = \Lambda(t+s, y)$ is used. Here and thereafter we assume that all relations (3.8)–(3.13) hold true.

Based on (3.8) and (3.9) we suggest the property:

(T1) Bijection holds between the function spaces

$$u \mapsto u \circ \phi_s^{-1} : V(\Omega_t) \mapsto V(\Omega_{t+s}), \quad \tilde{u} \mapsto \tilde{u} \circ \phi_s : V(\Omega_{t+s}) \mapsto V(\Omega_t). \tag{3.14}$$

As the consequence of (T1), for $(\tilde{u}, \tilde{v}) \in V(\Omega_{t+s})^2$ the perturbed Lagrangian in (3.3) is well defined after transformation to the reference geometry Ω_t by setting

$$\tilde{\mathcal{L}}^\varepsilon(s, u_t^\varepsilon, \tilde{u} \circ \phi_s, \tilde{v} \circ \phi_s; \Omega_t) := \tilde{\mathcal{L}}^\varepsilon(0, u_t^\varepsilon \circ \phi_s^{-1}, \tilde{u}, \tilde{v}; \Omega_{t+s}). \tag{3.15}$$

Applying the coordinate transformation (3.9) we calculate it in the explicit form

$$\begin{aligned} \tilde{\mathcal{L}}^\varepsilon(s, u_t^\varepsilon, u, v; \Omega_t) &= \frac{1}{2} \int_{\Gamma_t^D} |u - z \circ \phi_s|^2 \omega_s^b dS_x + \rho \int_{\Sigma_t} \omega_s^b dS_x \\ &\quad - \int_{\Omega \setminus \Sigma_t} ((C \circ \phi_s) E(\nabla \phi_s^{-1} \circ \phi_s, u) \cdot E(\nabla \phi_s^{-1} \circ \phi_s, v)) \omega_s^d dx \\ &\quad + \int_{\Gamma_t^N} (g \circ \phi_s) \cdot v \omega_s^b dS_x - \int_{\Sigma_t} \left\{ \alpha [[u]]_{\tilde{\tau}_{t+s}} \cdot [[v]]_{\tilde{\tau}_{t+s}} + [\alpha \tilde{v}_{t+s} \cdot [[u]] \right. \\ &\quad \left. + \int_0^1 \beta'_\varepsilon(\tilde{v}_{t+s} \cdot [[ru_t^\varepsilon]]) (\tilde{v}_{t+s} \cdot [[u]]) dr + \beta_\varepsilon(0) \right] (\tilde{v}_{t+s} \cdot [[v]]) \Big\} \omega_s^b dS_x \end{aligned} \tag{3.16}$$

for $(u, v) \in V(\Omega_t)^2$, see [30, 32], where the Jacobian determinants are

$$\omega_s^d := \det(\nabla \phi_s) \text{ in } \Omega \setminus \Sigma_t, \quad \omega_s^b := |(\nabla \phi_s^{-T} \circ \phi_s) n_t^\pm| \omega_s^d \text{ at } \partial\Omega_t^\pm. \quad (3.17)$$

Here the following decomposition at Σ_t was used akin to (2.1):

$$[[u]] = (\tilde{\nu}_{t+s} \cdot [[u]]) \tilde{\nu}_{t+s} + [[u]]_{\tilde{\tau}_{t+s}}, \quad \tilde{\nu}_{t+s} := \nu_{t+s} \circ \phi_s, \quad (3.18)$$

and the generalized strain for which $E(I, u) = \epsilon(u)$ according to (2.3):

$$E(M, u) := \frac{1}{2}(M^T \nabla u + \nabla u^T M), \quad M \in \mathbb{R}^{d \times d} \quad (3.19)$$

appears in view of the chain rule $\nabla_y \tilde{u} = (\nabla \phi_s^{-T} \circ \phi_s) \nabla(\tilde{u} \circ \phi_s)$.

(T2) Partial derivative of $\tilde{\mathcal{L}}^\epsilon$ from (3.16) in the first argument exists as $s \rightarrow 0$:

$$\tilde{\mathcal{L}}^\epsilon(s, u_t^\epsilon, u, v; \Omega_t) = \tilde{\mathcal{L}}^\epsilon(0, u_t^\epsilon, u, v; \Omega_t) + s \frac{\partial}{\partial s} \tilde{\mathcal{L}}^\epsilon(0, u_t^\epsilon, u, v; \Omega_t) + o(|s|) \quad (3.20)$$

given by the explicit representation, which is continuous in τ :

$$\begin{aligned} \frac{\partial}{\partial s} \tilde{\mathcal{L}}^\epsilon(\tau, u_t^\epsilon, u, v; \Omega_t) &= \rho \int_{\Sigma_t} \operatorname{div}_{\tau_t} \Lambda|_{t+\tau} dS_x \\ &+ \int_{\Gamma_t^0} \left(\frac{1}{2} \operatorname{div}_{\tau_t} \Lambda|_{t+\tau} |u-z|^2 - \nabla z \Lambda|_{t+\tau} \cdot (u-z) \right) dS_x \\ &+ \int_{\Omega \setminus \Sigma_t} I(\Omega \setminus \Sigma_{t+\tau}) dx + \int_{\Gamma_t^N} (\operatorname{div}_{\tau_t} \Lambda|_{t+\tau} g + \nabla g \Lambda|_{t+\tau}) \cdot v dS_x \\ &- \int_{\Sigma_t} \left\{ \alpha [[u]]_{\nabla_{\tau_t} \Lambda|_{t+\tau}} \cdot [[v]]_{\tau_t} dr + \alpha [[u]]_{\tau_t} \cdot (\operatorname{div}_{\tau_t} \Lambda|_{t+\tau} [[v]]_{\tau_t} + [[v]]_{\nabla_{\tau_t} \Lambda|_{t+\tau}}) \right. \\ &+ \left(\int_0^1 \beta'_\epsilon(\nu_t \cdot [[ru_t^\epsilon]]) (\nu_t \cdot [[u]]) dr + \beta_\epsilon(0) \right) \left((\operatorname{div}_{\tau_t} \Lambda|_{t+\tau} \nu_t \right. \\ &\left. + \nabla \nu_t \Lambda|_{t+\tau}) \cdot [[v]] \right) + \int_0^1 \beta'_\epsilon(\nu_t \cdot [[ru_t^\epsilon]]) (\nabla \nu_t \Lambda|_{t+\tau} \cdot [[u]]) (\nu_t \cdot [[v]]) dr \left. \right\} dS_x. \end{aligned} \quad (3.21)$$

Here the notation

$$\begin{aligned} I(\Omega \setminus \Sigma_{t+\tau}) &:= -(\operatorname{div} \Lambda|_{t+\tau} C + \nabla C \Lambda|_{t+\tau}) \epsilon(u) \cdot \epsilon(v) \\ &+ \sigma(u) \cdot E(\nabla \Lambda|_{t+\tau}, v) + \sigma(v) \cdot E(\nabla \Lambda|_{t+\tau}, u), \end{aligned}$$

the tangential divergence $\operatorname{div}_{\tau_t} \Lambda = \operatorname{div} \Lambda - (\nabla \Lambda n_t^\pm) \cdot n_t^\pm$ at $\partial\Omega_t^\pm$, and

$$\begin{aligned} [[u]]_{\nabla_{\tau_t} \Lambda} &:= -(\nu_t \cdot [[u]]) \nabla \nu_t \Lambda - (\nabla \nu_t \Lambda \cdot [[u]]) \nu_t, \\ \nabla \nu_t \Lambda &:= ((\nabla \Lambda \nu_t) \cdot \nu_t) \nu_t - \nabla \Lambda^T \nu_t \quad \text{at } \Sigma_t. \end{aligned} \quad (3.22)$$

Proof. As $s \rightarrow 0$, the following asymptotic expansion holds (see e.g. [44, chapter 2]):

$$\begin{aligned} z \circ \phi_s &= z + s \nabla z \Lambda + o(s), \quad g \circ \phi_s = g + s \nabla g \Lambda + o(s), \\ C \circ \phi_s &= g + s \nabla C \Lambda + o(s), \quad \nabla \phi_s^{-1} \circ \phi_s = I - s \nabla \Lambda + o(s), \\ E(\nabla \phi_s^{-1} \circ \phi_s, u) &= \epsilon(u) - s E(\nabla \Lambda, u) + o(s), \\ \omega_s^d &= 1 + s \operatorname{div} \Lambda + o(s), \quad \omega_s^b = 1 + s \operatorname{div}_{\tau_t} \Lambda + o(s) \\ \nu_{t+s} \circ \phi_s &= \nu_t + s \nabla \nu_t \Lambda + o(s), \quad [[u]]_{\tilde{\tau}_{t+s}} = [[u]]_{\tau_t} + s [[u]]_{\nabla_{\tau_t} \Lambda} + o(s) \end{aligned} \quad (3.23)$$

for $u \in V(\Omega_t)$, using the equations (3.12), (3.13) and notation (3.22). Substituting (3.23) into representations (3.16)–(3.19) of the perturbed Lagrangian follows the expansion (3.20) with the asymptotic term $\frac{\partial}{\partial s} \tilde{\mathcal{L}}^\epsilon(0, u_t^\epsilon, u, v; \Omega_t)$ from (3.21) at $\tau=0$ and $\Lambda|_t = \Lambda$. Since $\Lambda|_{t+\tau}$ and

$\nabla\Lambda|_{t+\tau}$ are continuous functions of the argument $t + \tau$, the partial derivative in (3.21) is continuous in the first argument τ . □

We look for a perturbed saddle-point problem: find $(\tilde{u}_{t+s}^\varepsilon, \tilde{v}_{t+s}^\varepsilon) \in V(\Omega_t)^2$ satisfying

$$\tilde{\mathcal{L}}^\varepsilon(s, u_t^\varepsilon, \tilde{u}_{t+s}^\varepsilon, v; \Omega_t) \leq \tilde{\mathcal{L}}^\varepsilon(s, u_t^\varepsilon, \tilde{u}_{t+s}^\varepsilon, \tilde{v}_{t+s}^\varepsilon; \Omega_t) \leq \tilde{\mathcal{L}}^\varepsilon(s, u_t^\varepsilon, u, \tilde{v}_{t+s}^\varepsilon; \Omega_t) \tag{3.24}$$

for all $(u, v) \in V(\Omega_t)^2$. The problem coincides with (3.4) at $s = 0$.

(T3) Saddle point $(\tilde{u}_{t+s}^\varepsilon, \tilde{v}_{t+s}^\varepsilon) \in V(\Omega_t)^2$ in (3.24) exists at $s \in (-s_0, s_0) \cap I$ at least for small $s_0 > 0$, it is unique, and $(\tilde{u}_t^\varepsilon, \tilde{v}_t^\varepsilon) = (u_t^\varepsilon, v_t^\varepsilon)$ at $s = 0$.

Proof. The perturbed Lagrangian $\tilde{\mathcal{L}}^\varepsilon(s)$ in (3.16) is quadratic and convex in u , and linear in v . The optimality condition $\partial_v \tilde{\mathcal{L}}^\varepsilon(s, u_t^\varepsilon, \tilde{u}_{t+s}^\varepsilon, \tilde{v}_{t+s}^\varepsilon; \Omega_t) = 0$ implies

$$\begin{aligned} & \int_{\Omega \setminus \Sigma_t} ((C \circ \phi_s) E(\nabla \phi_s^{-1} \circ \phi_s, \tilde{u}_{t+s}^\varepsilon) \cdot E(\nabla \phi_s^{-1} \circ \phi_s, u)) \omega_s^d dx \tag{3.25} \\ & + \int_{\Sigma_t} \left\{ \alpha [[\tilde{u}_{t+s}^\varepsilon]]_{\tilde{\tau}_{t+s}} \cdot [[u]]_{\tilde{\tau}_{t+s}} + \left[\alpha \tilde{v}_{t+s} \cdot [[\tilde{u}_{t+s}^\varepsilon]] + \int_0^1 \beta'_\varepsilon(\tilde{v}_{t+s} \cdot [[ru_t^\varepsilon]]) \right. \right. \\ & \left. \left. \times (\tilde{v}_{t+s} \cdot [[\tilde{u}_{t+s}^\varepsilon]]) dr + \beta_\varepsilon(0) \right] (\tilde{v}_{t+s} \cdot [[u]]) \right\} \omega_s^b dS_x = \int_{\Gamma_t^N} (g \circ \phi_s) \cdot u \omega_s^b dS_x \end{aligned}$$

for all $u \in V(\Omega_t)$. Due to the asymptotic representation in (T2) and the mean value theorem, the equation (3.25) can be expressed using the operator A_ε from (3.6) as

$$\langle A_\varepsilon(u_t^\varepsilon) \tilde{u}_{t+s}^\varepsilon, u \rangle + \int_{\Sigma_t} \beta_\varepsilon(0) (\nu_t \cdot [[u]]) dS_x = \int_{\Gamma_t^N} g \cdot u dS_x + s R_v(\alpha_s^v, \tilde{u}_{t+s}^\varepsilon, u) \tag{3.26}$$

with weight $\alpha_s^v \in (0, s)$ and bounded bilinear residual $R_v : V(\Omega_t)^2 \mapsto \mathbb{R}$. The operator $A_\varepsilon(u_t^\varepsilon)$ is coercive and weakly continuous. By the Brouwer fixed point theorem, for ε small enough the variational equation (3.26) has a unique solution $\tilde{u}_{t+s}^\varepsilon \in V(\Omega_t)$.

The other optimality condition $\partial_u \tilde{\mathcal{L}}^\varepsilon(s, u_t^\varepsilon, \tilde{u}_{t+s}^\varepsilon, \tilde{v}_{t+s}^\varepsilon; \Omega_t) = 0$ has the form

$$\begin{aligned} & \int_{\Omega \setminus \Sigma_t} ((C \circ \phi_s) E(\nabla \phi_s^{-1} \circ \phi_s, v) \cdot E(\nabla \phi_s^{-1} \circ \phi_s, \tilde{v}_{t+s}^\varepsilon)) \omega_s^d dx \tag{3.27} \\ & + \int_{\Sigma_t} \left\{ \alpha [[\tilde{v}_{t+s}^\varepsilon]]_{\tilde{\tau}_{t+s}} \cdot [[v]]_{\tilde{\tau}_{t+s}} + \left[\alpha \tilde{v}_{t+s} \cdot [[\tilde{v}_{t+s}^\varepsilon]] + \int_0^1 \beta'_\varepsilon(\tilde{v}_{t+s} \cdot [[ru_t^\varepsilon]]) \right. \right. \\ & \left. \left. \times (\tilde{v}_{t+s} \cdot [[\tilde{v}_{t+s}^\varepsilon]]) dr \right] (\tilde{v}_{t+s} \cdot [[v]]) \right\} \omega_s^b dS_x = \int_{\Gamma_t^0} v \cdot (\tilde{u}_{t+s}^\varepsilon - z \circ \phi_s) \omega_s^b dS_x \end{aligned}$$

for all $v \in V(\Omega_t)$, which admits the asymptotic decomposition as

$$\langle A_\varepsilon(u_t^\varepsilon) v, \tilde{v}_{t+s}^\varepsilon \rangle = \int_{\Gamma_t^0} v \cdot (\tilde{u}_{t+s}^\varepsilon - z) dS_x + s R_u(\alpha_s^u, v, \tilde{v}_{t+s}^\varepsilon) \tag{3.28}$$

with weight $\alpha_s^u \in (0, s)$ and bounded bilinear residual $R_u : V(\Omega_t)^2 \mapsto \mathbb{R}$. Its unique solution $\tilde{v}_{t+s}^\varepsilon \in V(\Omega_t)$ is guaranteed at least for small s . This finishes the proof. □

(T4) Strongly convergent subsequence for $k \rightarrow \infty$ exists such that

$$(\tilde{u}_{t+s_k}^\varepsilon, \tilde{v}_{t+s_k}^\varepsilon) \rightarrow (u_t^\varepsilon, v_t^\varepsilon) \text{ strongly in } V(\Omega_t)^2 \text{ as } s_k \rightarrow 0. \tag{3.29}$$

Proof. The proof is split into the three steps: uniform estimate, weak convergence, and strong convergence.

Uniform estimate. We test the primal equation (3.25) with $u = \tilde{u}_{t+s}^\varepsilon$ and use (3.26):

$$\begin{aligned} & \int_{\Omega \setminus \Sigma_t} \sigma(\tilde{u}_{t+s}^\varepsilon) \cdot \epsilon(\tilde{u}_{t+s}^\varepsilon) \, dx + \int_{\Sigma_t} \left\{ \alpha |[\![\tilde{u}_{t+s}^\varepsilon]\!]|^2 \right. \\ & \quad \left. + \int_0^1 \beta'_\varepsilon(\nu_t \cdot [\![ru_t^\varepsilon]\!]) \, dr (\nu_t \cdot [\![\tilde{u}_{t+s}^\varepsilon]\!])^2 + \beta_\varepsilon(0)(\nu_t \cdot [\![\tilde{u}_{t+s}^\varepsilon]\!]) \right\} dS_x \\ & = \int_{\Gamma_t^N} g \cdot \tilde{u}_{t+s}^\varepsilon \, dS_x + sR_v(\alpha_s^v, \tilde{u}_{t+s}^\varepsilon, \tilde{u}_{t+s}^\varepsilon), \end{aligned} \tag{3.30}$$

then apply the Cauchy–Schwarz, Korn–Poincaré (2.4) and trace (2.17) inequalities. By the virtue of $\beta'_\varepsilon \geq 0$ and $\beta_\varepsilon(0) = -\exp(-2)$ in (2.12), it follows the estimate:

$$\begin{aligned} & (K_{KP} - C_1|s|) \|\tilde{u}_{t+s}^\varepsilon\|_{H^1(\Omega \setminus \Sigma_t)^d} + \alpha \|[\![\tilde{u}_{t+s}^\varepsilon]\!]\|_{L^2(\Sigma_t)^d} \\ & \leq K_{tr} (\|g\|_{L^2(\Gamma_t^N)^d} - \beta_\varepsilon(0) \sqrt{2|\Sigma_t|}) + C_1|s|, \quad C_1 > 0, \end{aligned} \tag{3.31}$$

which is uniform in ε and $|s| \leq s_0$ for $s_0 > 0$ sufficiently small.

Similarly, the adjoint equation (3.27) tested with $v = \tilde{v}_{t+s}^\varepsilon$ and (3.28) gives

$$\begin{aligned} & \int_{\Omega \setminus \Sigma_t} \sigma(\tilde{v}_{t+s}^\varepsilon) \cdot \epsilon(\tilde{v}_{t+s}^\varepsilon) \, dx + \int_{\Sigma_t} \left\{ \alpha |[\![\tilde{v}_{t+s}^\varepsilon]\!]|^2 + \int_0^1 \beta'_\varepsilon(\nu_t \cdot [\![ru_t^\varepsilon]\!]) \, dr \right. \\ & \quad \left. \times (\nu_t \cdot [\![\tilde{v}_{t+s}^\varepsilon]\!])^2 \right\} dS_x = \int_{\Gamma_t^0} \tilde{v}_{t+s}^\varepsilon \cdot (\tilde{u}_{t+s}^\varepsilon - z) \, dS_x + sR_u(\alpha_s^u, \tilde{v}_{t+s}^\varepsilon, \tilde{v}_{t+s}^\varepsilon) \end{aligned} \tag{3.32}$$

which follows the uniform bound:

$$\begin{aligned} & (K_{KP} - C_2|s|) \|\tilde{v}_{t+s}^\varepsilon\|_{H^1(\Omega \setminus \Sigma_t)^d} + \alpha \|[\![\tilde{v}_{t+s}^\varepsilon]\!]\|_{L^2(\Sigma_t)^d} \\ & \leq K_{tr} \|\tilde{u}_{t+s}^\varepsilon - z\|_{L^2(\Gamma_t^0)^d} + C_2|s|, \quad C_2 > 0. \end{aligned} \tag{3.33}$$

For small $s_0 < K_{KP} / \min(C_1, C_2)$ the estimates (3.32) and (3.33) together provide

$$\|\tilde{u}_{t+s}^\varepsilon\|_{H^1(\Omega \setminus \Sigma_t)^d} + \|\tilde{v}_{t+s}^\varepsilon\|_{H^1(\Omega \setminus \Sigma_t)^d} \leq K, \quad K \geq 0, \quad |s| \leq s_0. \tag{3.34}$$

Weak convergence. From the uniform estimate (3.34) we conclude with a subsequence $s_k \rightarrow 0$ as $k \rightarrow \infty$ and a weak accumulation point $(\tilde{u}_t^\varepsilon, \tilde{v}_t^\varepsilon) \in V(\Omega_t)^2$ such that

$$(\tilde{u}_{t+s_k}^\varepsilon, \tilde{v}_{t+s_k}^\varepsilon) \rightharpoonup (\tilde{u}_t^\varepsilon, \tilde{v}_t^\varepsilon) \quad \text{weakly in } H^1(\Omega \setminus \Sigma_t)^{2d}, H^{1/2}(\partial\Omega_t^\pm)^{2d}. \tag{3.35}$$

By the compactness of embedding for the space of boundary traces it follows

$$(\tilde{u}_{t+s_k}^\varepsilon, \tilde{v}_{t+s_k}^\varepsilon) \rightarrow (\tilde{u}_t^\varepsilon, \tilde{v}_t^\varepsilon) \quad \text{strongly in } L^2(\partial\Omega_t^\pm)^{2d} \text{ as } s_k \rightarrow 0. \tag{3.36}$$

Taking the limit as $k \rightarrow \infty$ in (3.26) and (3.28) for $s = s_k$, based on the convergences (3.35) and (3.36), uniform continuity of β'_ε , and identity (3.2), we arrive at the variational equations (2.15) and (3.6), thus, $(\tilde{u}_t^\varepsilon, \tilde{v}_t^\varepsilon) = (u_t^\varepsilon, v_t^\varepsilon)$.

Strong convergence. We test the primal variational equation (2.15) with $u = u_t^\varepsilon$ and apply the identity (3.2) such that

$$\begin{aligned} & \int_{\Omega \setminus \Sigma_t} \sigma(u_t^\varepsilon) \cdot \epsilon(u_t^\varepsilon) \, dx + \int_{\Sigma_t} \left\{ \alpha |[\![u_t^\varepsilon]\!]|^2 + \int_0^1 \beta'_\varepsilon(\nu_t \cdot [\![ru_t^\varepsilon]\!]) \, dr \right. \\ & \quad \left. \times (\nu_t \cdot [\![u_t^\varepsilon]\!])^2 + \beta_\varepsilon(0)(\nu_t \cdot [\![u_t^\varepsilon]\!]) \right\} dS_x = \int_{\Gamma_t^N} g \cdot u_t^\varepsilon \, dS_x. \end{aligned} \tag{3.37}$$

After subtraction of (3.37) from the asymptotic relation (3.30), with the help of the Korn–Poincaré inequality (2.4) we rearrange the terms as follows

$$\begin{aligned} K_{\text{KP}} \|\tilde{u}_{t+s}^\varepsilon - u_t^\varepsilon\|_{H^1(\Omega \setminus \Sigma_t)}^2 &\leq \int_{\Omega \setminus \Sigma_t} \sigma(\tilde{u}_{t+s}^\varepsilon - u_t^\varepsilon) \cdot \epsilon(\tilde{u}_{t+s}^\varepsilon - u_t^\varepsilon) dx \\ &= \int_{\Gamma_t^N} g \cdot (\tilde{u}_{t+s}^\varepsilon - u_t^\varepsilon) dS_x - 2 \int_{\Omega \setminus \Sigma_t} \sigma(\tilde{u}_{t+s}^\varepsilon - u_t^\varepsilon) \cdot \epsilon(u_t^\varepsilon) dx \\ &\quad - \int_{\Sigma_t} \left\{ \alpha \left(|\llbracket \tilde{u}_{t+s}^\varepsilon \rrbracket|^2 - |\llbracket u_t^\varepsilon \rrbracket|^2 \right) + \int_0^1 \beta'_\varepsilon(\nu_t \cdot \llbracket ru_t^\varepsilon \rrbracket) dr \right. \\ &\quad \left. \times \left((\nu_t \cdot \llbracket \tilde{u}_{t+s}^\varepsilon \rrbracket)^2 - (\nu_t \cdot \llbracket u_t^\varepsilon \rrbracket)^2 \right) + \beta_\varepsilon(0) (\nu_t \cdot \llbracket \tilde{u}_{t+s}^\varepsilon - u_t^\varepsilon \rrbracket) \right\} dS_x + O(|s|). \end{aligned} \quad (3.38)$$

The limit in (3.38) due to (3.35) and (3.36) leads to the convergence of the norm

$$\|\tilde{u}_{t+s_k}^\varepsilon - u_t^\varepsilon\|_{H^1(\Omega \setminus \Sigma_t)} \rightarrow 0 \quad \text{as } s_k \rightarrow 0. \quad (3.39)$$

Now we subtract the adjoint equation (3.6) from (3.28):

$$\begin{aligned} \int_{\Omega \setminus \Sigma_t} \epsilon(v) \cdot \sigma(\tilde{v}_{t+s}^\varepsilon - v_t^\varepsilon) dx &= \int_{\Gamma_t^0} (\tilde{v}_{t+s}^\varepsilon - v_t^\varepsilon) \cdot \nu dS_x - \int_{\Sigma_t} \left\{ \alpha \llbracket \tilde{v}_{t+s}^\varepsilon - v_t^\varepsilon \rrbracket \right. \\ &\quad \left. \cdot \llbracket v \rrbracket + \int_0^1 \beta'_\varepsilon(\nu \cdot \llbracket ru_t^\varepsilon \rrbracket) (\nu \cdot \llbracket \tilde{v}_{t+s}^\varepsilon - v_t^\varepsilon \rrbracket) dr \right\} (\nu \cdot \llbracket v \rrbracket) \Big\} dS_x + O(|s|). \end{aligned} \quad (3.40)$$

Then the Korn–Poincaré (2.4) and trace (2.17) inequalities together with convergences (3.35) and (3.36) applied to (3.40) guarantees zero limit in the strong topology:

$$\begin{aligned} K_{\text{KP}} \|\tilde{v}_{t+s_k}^\varepsilon - v_t^\varepsilon\|_{H^1(\Omega \setminus \Sigma_t)} & \\ &\leq \sup_{v \in V(\Omega_t)} \frac{1}{\|v\|_{H^1(\Omega \setminus \Sigma_t)}} \int_{\Omega \setminus \Sigma_t} \epsilon(v) \cdot \sigma(v_{t+s_k}^\varepsilon - v_t^\varepsilon) dx \rightarrow 0 \end{aligned} \quad (3.41)$$

as $s_k \rightarrow 0$. The proof is complete. \square

Based on (T1)–(T4), all assumptions in [11, chapter 10, theorem 5.1] are satisfied, thus establishing the following theorem (see details of the proof in [33]).

Theorem 4 (Shape gradient). *A shape gradient for the perturbed Lagrangian exists given by the partial derivative $\frac{\partial}{\partial s} \tilde{\mathcal{L}}^\varepsilon$ from (3.21):*

$$\begin{aligned} \lim_{s \rightarrow 0^+} \frac{1}{s} \left(\tilde{\mathcal{L}}^\varepsilon(s, u_t^\varepsilon, \tilde{u}_{t+s}^\varepsilon, \tilde{v}_{t+s}^\varepsilon; \Omega_t) - \tilde{\mathcal{L}}^\varepsilon(0, u_t^\varepsilon, u_t^\varepsilon, v_t^\varepsilon; \Omega_t) \right) \\ = \frac{\partial}{\partial s} \tilde{\mathcal{L}}^\varepsilon(0, u_t^\varepsilon, u_t^\varepsilon, v_t^\varepsilon; \Omega_t) \end{aligned} \quad (3.42)$$

at the saddle-point $(u_t^\varepsilon, v_t^\varepsilon) \in V(\Omega_t)^2$ from (3.4).

In the next theorem we calculate the specific boundary expression of $\frac{\partial}{\partial s} \tilde{\mathcal{L}}^\varepsilon$ according to the Hadamard structure of shape gradients defined on submanifolds as stated in the abstract theorem by [34, proposition 4.3].

Theorem 5 (Hadamard representation). *Let the solutions of (2.15) and (3.6) be smooth $(u_t^\varepsilon, v_t^\varepsilon) \in H^2(\Omega_t^+) \cap H^2(\Omega_t^-)$. Decomposing as*

$$\Lambda = (n_t \cdot \Lambda)n_t + \Lambda_{\tau_t}, \quad \nabla = (n_t \cdot \nabla)n_t + \nabla_{\tau_t}, \quad \mathcal{D} = (n_t \cdot \mathcal{D})n_t + \mathcal{D}_{\tau_t} \quad (3.43)$$

the shape gradient in (3.42) equals to the sum of boundary integrals

$$\begin{aligned} \frac{\partial}{\partial s} \tilde{\mathcal{L}}^\varepsilon(0, u_t^\varepsilon, v_t^\varepsilon; \Omega_t) &= \int_{\Gamma_t^p} (\tau_t \cdot \Lambda) \tau_t \cdot \mathcal{D}_1(u_t^\varepsilon, v_t^\varepsilon) dS_x \\ &+ \int_{\Sigma_t} \left\{ (\tau_t \cdot \Lambda) \tau_t \cdot \mathcal{D}_2^\varepsilon(u_t^\varepsilon, v_t^\varepsilon) + (\nu_t \cdot \Lambda) \mathcal{D}_3^\varepsilon(u_t^\varepsilon, v_t^\varepsilon) \right\} dS_x + B, \end{aligned} \quad (3.44)$$

where the term B is given in 2D by

$$B = (\tau_t \cdot \Lambda) [\mathcal{D}_4^\varepsilon(u_t^\varepsilon, v_t^\varepsilon)]_{\partial \Sigma_t} + (\tau_t \cdot \Lambda) \mathcal{D}_5(u_t^\varepsilon)|_{\partial \Gamma_t^o} + (\tau_t \cdot \Lambda) [\mathcal{D}_6(v_t^\varepsilon)]_{\partial \Gamma_t^N \cap \Sigma_t}, \quad (3.45)$$

for tangential vector τ_t at the boundary, and in 3D by

$$\begin{aligned} B &= \int_{\partial \Sigma_t} (b_t \cdot \Lambda) [\mathcal{D}_4^\varepsilon(u_t^\varepsilon, v_t^\varepsilon)] dL_x \\ &+ \int_{\partial \Gamma_t^o} (b_t \cdot \Lambda) \mathcal{D}_5(u_t^\varepsilon) dL_x + \int_{\partial \Gamma_t^N \cap \Sigma_t} (b_t \cdot \Lambda) [\mathcal{D}_6(v_t^\varepsilon)] dL_x \end{aligned} \quad (3.46)$$

for the binomial vector $b_t = \tau_t \times n_t$ within moving frame. The expressions are

$$\begin{aligned} \mathcal{D}_1(u, v) &:= \nabla u^\top \sigma(v) n_t + \nabla v^\top \sigma(u) n_t, \quad \mathcal{D}_2^\varepsilon(u, v) := -q^\varepsilon(u, v), \\ \mathcal{D}_3^\varepsilon(u, v) &:= [\sigma(u) \cdot \epsilon(v)] + \rho \varkappa_t - \varkappa_t p^\varepsilon(u, v) - \nu_t \cdot [\nabla p^\varepsilon + q^\varepsilon](u, v), \\ \mathcal{D}_4^\varepsilon(u, v) &:= \rho - p^\varepsilon(u, v), \quad \mathcal{D}_5(u) := \frac{1}{2} |u - z|^2, \quad \mathcal{D}_6(v) := g \cdot v, \end{aligned} \quad (3.47)$$

with the curvature $\varkappa_t = \operatorname{div}_{\tau_t} \nu_t$ and notation

$$\begin{aligned} p^\varepsilon(u, v) &:= \alpha [[u]] \cdot [[v]] + \beta_\varepsilon (\nu_t \cdot [[u]]) (\nu_t \cdot [[v]]), \\ q^\varepsilon(u, v) &:= \nabla (\nu_t \cdot [[u]])^\top \left(\int_0^1 \beta'_\varepsilon (\nu_t \cdot [[ru_t^\varepsilon]]) dr - \beta'_\varepsilon (\nu_t \cdot [[u_t^\varepsilon]]) \right) (\nu_t \cdot [[v]]). \end{aligned} \quad (3.48)$$

Proof. We integrate by parts over domain $\Omega \setminus \Sigma_t$ the integrand $I(\Omega \setminus \Sigma_t)$ from (3.21) at $\tau = 0$. Using the assumption $n_t \cdot \Lambda = 0$ at $\partial \Omega$, notation \mathcal{D}_1 from (3.47), boundary conditions (2.16b)–(2.16f) and (3.7b)–(3.7g) it follows that

$$\begin{aligned} \int_{\Omega \setminus \Sigma_t} I(\Omega \setminus \Sigma_t) dx &= \int_{\Sigma_t} \Lambda \cdot \left\{ \nu_t [\sigma(u_t^\varepsilon) \cdot \epsilon(v_t^\varepsilon)] \right. \\ &- [\nabla v_t^\varepsilon]^\top \left(\alpha [[u_t^\varepsilon]] + \beta_\varepsilon (\nu_t \cdot [[u_t^\varepsilon]]) \nu_t \right) - [[\nabla u_t^\varepsilon]]^\top \left(\alpha [[u_t^\varepsilon]] \cdot [[v_t^\varepsilon]] \right. \\ &+ \left. \int_0^1 \beta'_\varepsilon (\nu_t \cdot [[ru_t^\varepsilon]]) dr (\nu_t \cdot [[v_t^\varepsilon]]) \nu_t \right\} dS_x + \int_{\Gamma_t^o} \Lambda \cdot \nabla (u_t^\varepsilon)^\top (u_t^\varepsilon - z) dS_x \\ &+ \int_{\Gamma_t^N} \Lambda \cdot \nabla (v_t^\varepsilon)^\top g dS_x + \int_{\Gamma_t^p} \Lambda \cdot \mathcal{D}_1(u_t^\varepsilon, v_t^\varepsilon) dS_x. \end{aligned} \quad (3.49)$$

After substitution of (3.49) into (3.21), the integrand at Σ_t is gathered as follows

$$\begin{aligned}
I_{\Sigma_t} := & -\operatorname{div}_{\tau} \Lambda \left\{ \alpha \llbracket u_t^\varepsilon \rrbracket \cdot \llbracket v_t^\varepsilon \rrbracket + \beta_\varepsilon (\nu_t \cdot \llbracket u_t^\varepsilon \rrbracket) (\nu_t \cdot \llbracket v_t^\varepsilon \rrbracket) \right\} \\
& + \Lambda \cdot \left\{ \nu_t \llbracket \sigma(u_t^\varepsilon) \cdot \epsilon(v_t^\varepsilon) \rrbracket - \left(\llbracket \nabla v_t^\varepsilon \rrbracket^\top - (\nu_t \cdot \llbracket v_t^\varepsilon \rrbracket) \nabla \nu_t^\top \right) \alpha \llbracket u_t^\varepsilon \rrbracket_{\tau} \right. \\
& - \left(\llbracket \nabla v_t^\varepsilon \rrbracket^\top \nu_t + \nabla \nu_t^\top \llbracket v_t^\varepsilon \rrbracket \right) [\alpha \operatorname{id} + \beta_\varepsilon] (\nu_t \cdot \llbracket u_t^\varepsilon \rrbracket) \\
& - \left(\llbracket \nabla u_t^\varepsilon \rrbracket^\top - (\nu_t \cdot \llbracket u_t^\varepsilon \rrbracket) \nabla \nu_t^\top \right) \alpha \llbracket v_t^\varepsilon \rrbracket_{\tau} \\
& \left. - \left(\llbracket \nabla u_t^\varepsilon \rrbracket^\top \nu_t + \nabla \nu_t^\top \llbracket u_t^\varepsilon \rrbracket \right) \left(\alpha + \int_0^1 \beta'_\varepsilon (\nu_t \cdot \llbracket r u_t^\varepsilon \rrbracket) dr \right) (\nu_t \cdot \llbracket v_t^\varepsilon \rrbracket) \right\}.
\end{aligned} \tag{3.50}$$

To combine like terms, we exploit the calculus for $\xi, \eta \in \mathbb{R}^d$:

$$\Lambda \cdot \nabla (\xi \cdot \eta) = \Lambda \cdot (\nabla \xi^\top \eta + \nabla \eta^\top \xi) = \eta \cdot \nabla \xi \Lambda + \xi \cdot \nabla \eta \Lambda. \tag{3.51}$$

With the help of (3.51), the gradient of p^ε from (3.48) is calculated as

$$\begin{aligned}
\nabla p^\varepsilon(u, v) = & \nabla (\llbracket v \rrbracket_{\tau})^\top \alpha \llbracket u \rrbracket_{\tau} + \nabla (\llbracket u \rrbracket_{\tau})^\top \alpha \llbracket v \rrbracket_{\tau} + \left(\llbracket \nabla \tilde{v} \rrbracket^\top \nu_t + \nabla \nu_t^\top \llbracket \tilde{v} \rrbracket \right) \\
& \times [\alpha \operatorname{id} + \beta_\varepsilon] (\nu_t \cdot \llbracket u \rrbracket) + \left(\llbracket \nabla u \rrbracket^\top \nu_t + \nabla \nu_t^\top \llbracket u \rrbracket \right) [\alpha + \beta'_\varepsilon (\nu_t \cdot \llbracket u \rrbracket)] (\nu_t \cdot \llbracket v \rrbracket),
\end{aligned}$$

and the integrand in (3.50) can be expressed as

$$\begin{aligned}
I_{\Sigma_t} = & -\operatorname{div}_{\tau} \Lambda p_c^\varepsilon(u_t^\varepsilon, v_t^\varepsilon) + \Lambda \cdot \left\{ \nu_t \llbracket \sigma(u_t^\varepsilon) \cdot \epsilon(v_t^\varepsilon) \rrbracket - \nabla p^\varepsilon(u_t^\varepsilon, v_t^\varepsilon) \right. \\
& \left. - \nabla (\nu_t \cdot \llbracket u_t^\varepsilon \rrbracket)^\top \left(\int_0^1 \beta'_\varepsilon (\nu_t \cdot \llbracket r u_t^\varepsilon \rrbracket) dr - \beta'_\varepsilon (\nu_t \cdot \llbracket u_t^\varepsilon \rrbracket) \right) (\nu_t \cdot \llbracket v_t^\varepsilon \rrbracket) \right\}.
\end{aligned} \tag{3.52}$$

Based on (3.52) we introduce the notation of q^ε in (3.48) and rearrange

$$\begin{aligned}
\frac{\partial}{\partial s} \tilde{\mathcal{L}}^\varepsilon(0, u_t^\varepsilon, u_t^\varepsilon, v_t^\varepsilon; \Omega_t) = & \frac{1}{2} \int_{\Gamma_t^0} \left(\operatorname{div}_{\tau} \Lambda |u_t^\varepsilon - z|^2 \right. \\
& + \Lambda \cdot \nabla (|u_t^\varepsilon - z|^2) \Big) dS_x + \int_{\Sigma_t} \left\{ \operatorname{div}_{\tau} \Lambda \left(\rho - p^\varepsilon(u_t^\varepsilon, v_t^\varepsilon) \right) \right. \\
& + \Lambda \cdot \left(\nu_t \llbracket \sigma(u_t^\varepsilon) \cdot \epsilon(v_t^\varepsilon) \rrbracket - [\nabla p^\varepsilon + q^\varepsilon](u_t^\varepsilon, v_t^\varepsilon) \right) \Big\} dS_x \\
& + \int_{\Gamma_t^N} \left(\operatorname{div}_{\tau} \Lambda (g \cdot v_t^\varepsilon) + \Lambda \cdot \nabla (g \cdot v_t^\varepsilon) \right) dS_x + \int_{\Gamma_t^p} \Lambda \cdot \mathcal{D}_1(u_t^\varepsilon, v_t^\varepsilon) dS_x.
\end{aligned} \tag{3.53}$$

Using the tangential velocity, tangential divergence, and curvature at $\partial\Omega_t^\pm$:

$$\Lambda_{\tau} = \Lambda - (n_t^\pm \cdot \Lambda) n_t^\pm, \quad \operatorname{div}_{\tau} \Lambda_{\tau} = \operatorname{div}_{\tau} \Lambda - (n_t^\pm \cdot \Lambda) \varkappa_t^\pm, \quad \varkappa_t^\pm = \operatorname{div}_{\tau} n_t^\pm,$$

for smooth ζ integration along a boundary $\Gamma_t \subset \partial\Omega_t^\pm$ is given by (see [44, (2.125)]):

$$\int_{\Gamma_t} (\operatorname{div}_{\tau} \Lambda \zeta + \Lambda \cdot \nabla \zeta) dS_x = \int_{\Gamma_t} (n_t \cdot \Lambda) (\varkappa_t \zeta + n_t \cdot \nabla \zeta) dS_x + P(\zeta). \tag{3.54}$$

In 2D, the value $P(\zeta) = (\tau_t \cdot \Lambda) \zeta|_{\partial\Gamma_t}$, and τ_t is a tangential vector at $\partial\Gamma_t$ positively oriented to n_t . In 3D, this implies $P(\zeta) = \int_{\partial\Gamma_t} (b_t \cdot \Lambda) \zeta dL_x$ and $b_t = \tau_t \times n_t$ is a binomial vector within the moving frame at $\partial\Gamma_t$. Applying (3.54) to (3.53), using decomposition in (3.43), and recalling that $v_t^\varepsilon = 0$ at $\partial\Gamma_t^N \cap \Gamma_t^D$, we conclude with (3.44)–(3.47). \square

As the corollary of theorem 5, a descent direction for the perturbed Lagrangian in (3.42) is provided by the kinematic velocity

$$\begin{aligned} n_t \cdot \Lambda &= 0 \text{ at } \partial\Omega, \quad \Lambda_{\tau_t} = -k_1 \mathcal{D}_1(u_t^\varepsilon, v_t^\varepsilon)_{\tau_t} \text{ at } \Gamma_t^D, \\ \Lambda_{\tau_t} &= -k_2 \mathcal{D}_2^\varepsilon(u_t^\varepsilon, v_t^\varepsilon)_{\tau_t} \text{ and } \nu_t \cdot \Lambda = -k_3 \mathcal{D}_3^\varepsilon(u_t^\varepsilon, v_t^\varepsilon) \text{ at } \Sigma_t, \end{aligned} \quad (3.55)$$

such that in 2D:

$$\begin{aligned} \tau_t \cdot \Lambda &= -k_4 \llbracket \mathcal{D}_4^\varepsilon(u_t^\varepsilon, v_t^\varepsilon) \rrbracket \text{ at } \partial\Sigma_t, \quad \tau_t \cdot \Lambda = -k_5 \mathcal{D}_5(u_t^\varepsilon) \text{ at } \partial\Gamma_t^O, \\ \tau_t \cdot \Lambda &= -k_6 \llbracket \mathcal{D}_6(v_t^\varepsilon) \rrbracket \text{ at } \partial\Gamma_t^N \cap \Sigma_t, \end{aligned} \quad (3.56)$$

and in 3D, respectively:

$$\begin{aligned} b_t \cdot \Lambda &= -k_4 \llbracket \mathcal{D}_4^\varepsilon(u_t^\varepsilon, v_t^\varepsilon) \rrbracket \text{ at } \partial\Sigma_t, \quad b_t \cdot \Lambda = -k_5 \mathcal{D}_5(u_t^\varepsilon) \text{ at } \partial\Gamma_t^O, \\ b_t \cdot \Lambda &= -k_6 \llbracket \mathcal{D}_6(v_t^\varepsilon) \rrbracket \text{ at } \partial\Gamma_t^N \cap \Sigma_t, \end{aligned} \quad (3.57)$$

with $k_i \geq 0$, $i = 1, \dots, 6$, and not all simultaneously equal to zero.

Finally, it is worth noting that the limit passage as $\varepsilon \rightarrow 0$ is possible in the penalized equations (2.15) and (3.6). However, we can pass to the limit neither in the Lagrangian $\tilde{\mathcal{L}}^\varepsilon$ in (3.3), nor in its partial derivative $\frac{\partial}{\partial s} \tilde{\mathcal{L}}^\varepsilon$ in (3.21) because of the lack of continuity for the nonlinear term $\beta'_\varepsilon(\nu_t \cdot \llbracket u_t^\varepsilon \rrbracket)$.

4. Identification of the breaking-line subject to contact with adhesion

For a numerical example in 2D, we identify the straight line

$$\Sigma = \{x_1 \in (0, 1), x_2 = \psi(x_1)\}, \quad \psi(x_1) = 0.2x_1 + 0.1, \quad (4.1)$$

which breaks the rectangle $\Omega = (0, 1) \times (0, 0.5)$ into two parts Ω^\pm . Let $\partial\Omega$ consist of the fixed left and right Dirichlet boundaries $\Gamma^D = \{x_1 \in \{0, 1\}, 0 < x_2 < 0.5\}$, upper and lower Neumann boundaries $\Gamma^N = \{0 < x_1 < 1, x_2 \in \{0, 0.5\}\}$, see figure 2. Assuming that an isotropic elastic body occupies Ω we set the Young modulus $E_Y = 73000$ (mPa) and Poisson ratio $\nu_P = 0.34$ providing the Lamé parameters $\mu_L = E_Y / (2(1 + \nu_P)) \approx 27239$ and $\lambda_L = 2\mu_L\nu_P / (1 - 2\nu_P) \approx 57882$. For the corresponding matrix of isotropic elastic coefficients C , the stress–strain relations are given by

$$\sigma_{ij} = 2\mu_L \epsilon_{ij} + \lambda_L (\epsilon_{11} + \epsilon_{22}) \delta_{ij}, \quad i, j = 1, 2. \quad (4.2)$$

The adhesion parameter is taken $\alpha = 0.1$ (mPa), and the boundary force

$$g_1 \equiv 0, \quad g_2(x_1, 0.5) = (1 - 1.75x_1)\mu_L, \quad g_2(x_1, 0) = -g_2(x_1, 0.5). \quad (4.3)$$

Reasoned by flat shapes of $\{\Sigma\}$ we approximate the normal component $\nu_t \cdot \llbracket u \rrbracket$ by $\llbracket u \rrbracket_2 := \llbracket u_2 \rrbracket$, and tangential $\llbracket u \rrbracket_{\tau_t} = \llbracket u \rrbracket_1 \tau_t$ by $\llbracket u \rrbracket_1 := \llbracket u_1 \rrbracket$. The true solution $z \in H^1(\Omega \setminus \Sigma)^2$ such that $z = 0$ on Γ^D and $\llbracket z \rrbracket_2 \geq 0$ on Σ satisfies the VI (2.10):

$$\int_{\Omega \setminus \Sigma} \sigma(z) \cdot \epsilon(u - z) dx + \alpha \int_{\Sigma} \llbracket z \rrbracket \cdot \llbracket u - z \rrbracket dS_x \geq \int_{\Gamma^N} g \cdot (u - z) dS_x \quad (4.4)$$

for all test functions $u \in H^1(\Omega \setminus \Sigma)^2$ such that $u = 0$ on Γ^D and $\llbracket u \rrbracket_2 \geq 0$ on Σ . After finite element (FE) discretization on MATLAB *initmesh* of size $h = 10^{-2}$, (4.4) is solved by a primal-dual active set (PDAS) iterative algorithm (see [23]). We plot in figure 4 the true numerical solution z_h achieved after three iterations of PDAS. In plot (a) the grid is presented in the current (deformed) configuration $x + z(x)$ for $x \in \Omega \setminus \Sigma$ under the traction prescribed at Γ^N by g from (4.3). An open part of Σ where $\llbracket z \rrbracket_2 > 0$ is complementary to the contact part where

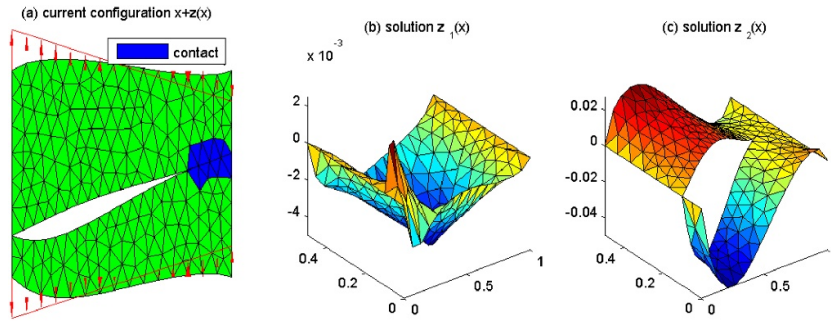


Figure 4. The true solution z_h with contact computed in current configuration (a) and componentwise (b), (c).

$[[z]]_2 = 0$, which is marked by dark elements adjacent to Σ . In plots (b) and (c) of figure 4, two solution components $(z_h)_1$ and $(z_h)_2$ are separately depicted in the reference configuration $x \in \Omega \setminus \Sigma$.

We consider a trial breaking-line $\Sigma_t \in \mathfrak{S}$ from the feasible set

$$\mathfrak{S} := \{x \in \Omega : x_1 \in (0, 1), x_2 = \psi(x_1) \in (0, 0.5), \psi \in C(0, 1)\}.$$

Let $V_{t,h}$ be the FE-space of piecewise-linear functions such that

$$V_{t,h} \subset V(\Omega_{t,h}) = \{u \in H^1(\Omega_{t,h}^+)^2 \cap H^1(\Omega_{t,h}^-)^2 \mid u = 0 \text{ on } \Gamma^D\}.$$

We solve the ε -penalized forward problem (2.15): find $u_{t,h}^\varepsilon \in V_{t,h}$ such that

$$\int_{\Omega \setminus \Sigma_{t,h}} \sigma(u_{t,h}^\varepsilon) \cdot \epsilon(u_h) dx + \int_{\Sigma_{t,h}} \left\{ \alpha [[u_{t,h}^\varepsilon]] \cdot [[u_h]] + (\beta_\varepsilon)_h ([[u_{t,h}^\varepsilon]]_2) [[u_h]]_2 \right\} dS_x = \int_{\Gamma^N} g \cdot u_h dS_x \quad (4.5)$$

for all $u_h \in V_{t,h}$. By this, we discretize the penalty function β_ε in (2.12) as

$$(\beta_\varepsilon)_h(s) = \frac{1}{\varepsilon} \min(0, s), \quad (\beta'_\varepsilon)_h(s) = \frac{1}{\varepsilon} \text{ind}\{s < 0\}. \quad (4.6)$$

The discrete adjoint equation (3.6) consists in finding $v_{t,h}^\varepsilon \in V_{t,h}$ such that

$$\int_{\Omega \setminus \Sigma_{t,h}} \sigma(v_h) \cdot \epsilon(v_{t,h}^\varepsilon) dx + \int_{\Sigma_{t,h}} \left\{ \alpha [[v_h]] \cdot [[v_{t,h}^\varepsilon]] + \int_0^1 (\beta'_\varepsilon)_h(r) [[ru_{t,h}^\varepsilon]]_2 dr [[v_h]]_2 [[v_{t,h}^\varepsilon]]_2 \right\} dS_x = \int_{\Gamma^O} v_h \cdot (u_{t,h}^\varepsilon - z_h) dS_x \quad (4.7)$$

for all test functions $v_h \in V_{t,h}$.

Assuming the observation boundary $\Gamma^O = \Gamma^N$, we synthesize the measurement z_h from (4.4) and consider the inverse problem of shape identification: find Σ_t such that

$$\min_{\Sigma_t \in \mathfrak{S}} \mathcal{J}(u_{t,h}^\varepsilon; \Omega_t) = \frac{1}{2} \int_{\Gamma^N} |u_{t,h}^\varepsilon - z_h|^2 dS_x + \rho |\Sigma_t| \quad (4.8)$$

where $u_{t,h}^\varepsilon$ solves (4.7). Zero minimum in (4.8) would be attained at $\Sigma_t = \Sigma$ and $u_{t,h}^\varepsilon = z_h$ without the contact and regularization. In this case, different meshes generated for z_h and $u_{t,h}^\varepsilon$ avoid the inverse crime.

After solving problems (4.5) and (4.7), according to the Hadamard representation (3.44) and (3.45) in 2D we calculate $\mathcal{D}_3^\varepsilon$ at the moving boundary $\Sigma_{t,h}$, and \mathcal{D}_1 at $\Sigma_{t,h} \cap \Gamma^D$, whereas Γ^D and Γ^N are fixed. From (3.47) we find the expressions

$$\begin{aligned} (\mathcal{D}_1)_{t,h} &= \llbracket \nabla(u_{t,h}^\varepsilon)^\top \sigma(v_{t,h}^\varepsilon) + \nabla(v_{t,h}^\varepsilon)^\top \sigma(u_{t,h}^\varepsilon) \rrbracket_2 \text{ at } x_1 = 1, \\ (\mathcal{D}_1)_{t,h} &= -\llbracket \nabla(u_{t,h}^\varepsilon)^\top \sigma(v_{t,h}^\varepsilon) + \nabla(v_{t,h}^\varepsilon)^\top \sigma(u_{t,h}^\varepsilon) \rrbracket_2 \text{ at } x_1 = 0, \\ (\mathcal{D}_3^\varepsilon)_{t,h} &= \llbracket \sigma(u_{t,h}^\varepsilon) \cdot \epsilon(v_{t,h}^\varepsilon) \rrbracket + \varkappa_t(\rho - p_{t,h}^\varepsilon) - \nu_t \cdot \nabla p_{t,h}^\varepsilon \end{aligned}$$

and set $\rho = 1/\mu_L$. From (3.48) we have $q_{t,h}^\varepsilon = 0$ by the virtue of (4.6), and the flat shape approximation $\nabla \nu_t = \nabla \tau_t = 0$ simplifies the gradient of $p_{t,h}^\varepsilon$ as

$$\begin{aligned} p_{t,h}^\varepsilon &= \alpha \llbracket u_{t,h}^\varepsilon \rrbracket \cdot \llbracket v_{t,h}^\varepsilon \rrbracket + (\beta_\varepsilon)_h(\llbracket u_{t,h}^\varepsilon \rrbracket_2) \llbracket v_{t,h}^\varepsilon \rrbracket_2, \quad \nabla p_{t,h}^\varepsilon = \llbracket \nabla v_{t,h}^\varepsilon \rrbracket_1^\top \alpha \llbracket u_{t,h}^\varepsilon \rrbracket_1 \\ &\quad + \llbracket \nabla v_{t,h}^\varepsilon \rrbracket_2^\top [\alpha \text{id} + (\beta_\varepsilon)_h(\llbracket u_{t,h}^\varepsilon \rrbracket_2)] + \llbracket \nabla u_{t,h}^\varepsilon \rrbracket_2^\top (\beta'_\varepsilon)_h(\llbracket u_{t,h}^\varepsilon \rrbracket_2) \llbracket v_{t,h}^\varepsilon \rrbracket_2. \end{aligned}$$

We define the discrete velocity Λ_H on a coarse grid of size $H > 0$ at Σ_t . For a descent direction, the velocity in (3.55) and (3.56) is determined by $(\Lambda_H)_1 = 0$ and

$$\begin{aligned} (\Lambda_H)_2 &= -k_3(\mathcal{D}_3^\varepsilon)_{t,h} \text{ on } \Sigma_{t,h} \setminus \Gamma^D, & (4.9) \\ (\Lambda_H)_2 &= -k_3(\mathcal{D}_3^\varepsilon)_{t,h} + k_1(1) \frac{k_3}{\sqrt{h}} ((\mathcal{D}_1)_{t,h})_2 \text{ on } \Sigma_{t,h} \cap \Gamma^D \text{ at } x_1 = 1, \\ (\Lambda_H)_2 &= -k_3(\mathcal{D}_3^\varepsilon)_{t,h} - k_1(0) \frac{k_3}{\sqrt{h}} ((\mathcal{D}_1)_{t,h})_2 \text{ on } \Sigma_{t,h} \cap \Gamma^D \text{ at } x_1 = 0, \end{aligned}$$

where the scaling $k_3 = 0.1h/\|(\Lambda_H)_2\|_{C(\overline{\Sigma_{t,h}})}$ is chosen, and the weight $1/\sqrt{h}$ at Γ^D was found empirically in [16]. For numerical consistency of the factors $k_1(x_1)$, $x_1 = 0, 1$ at $\Sigma_{t,h} \cap \Gamma^D$ in the last two lines in (4.9), we suggest $k_1(1) = 1$ if the contribution of $((\mathcal{D}_1)_{t,h})_2$ and $-(\mathcal{D}_3^\varepsilon)_{t,h}$ has the same sign at $x_1 = 1$, else $k_1(0) = 1$ if the signs of $-(\mathcal{D}_1)_{t,h})_2$ and $-(\mathcal{D}_3^\varepsilon)_{t,h}$ are same at $x_1 = 0$, otherwise $k_1(x_1) = 0$.

Based on the shape gradient we suggest the identification algorithm.

Algorithm 1 (Breaking-line identification)

- (0) Initialize at points $s_H \in [0, 1]$, e.g. the middle line $\psi_H^{(0)} \equiv 0.25$. Determine $\Sigma^{(0)} = \{x_1 \in (0, 1), x_2 = \psi^{(0)}(x_1)\}$ by the linear interpolate $\psi^{(0)}$ of $\psi_H^{(0)}$; set $n = 0$.
- (1) Set the breaking line $\Sigma_{t,h} = \Sigma^{(n)}$ and construct triangulations $\Omega_{t,h}^1, \Omega_{t,h}^2$; find solutions $u_{t,h}^\varepsilon, v_{t,h}^\varepsilon$ of the discrete penalty (4.5) and adjoint (4.7) equations.
- (2) Calculate a velocity $(\Lambda_H)_2$ by formula (4.9); update the grid function

$$\psi_H^{(n+1)} = \psi_H^{(n)} + (\Lambda_H)_2 \quad \text{at points } s_H \in [0, 1]. \tag{4.10}$$

From linear interpolation $\psi^{(n+1)}$ of $\psi_H^{(n+1)}$ determine the piecewise-linear segment

$$\Sigma^{(n+1)} = \{x_1 \in (0, 1), x_2 = \psi^{(n+1)}(x_1)\}. \tag{4.11}$$

- (3) If stopping criterion holds, then STOP; else set $n = n + 1$ and go to Step (1).

For equidistant points s_H as $H = 0.1$, the numerical result of Algorithm 1 stopped after $\#n = 200$ iterations is depicted in figure 5.

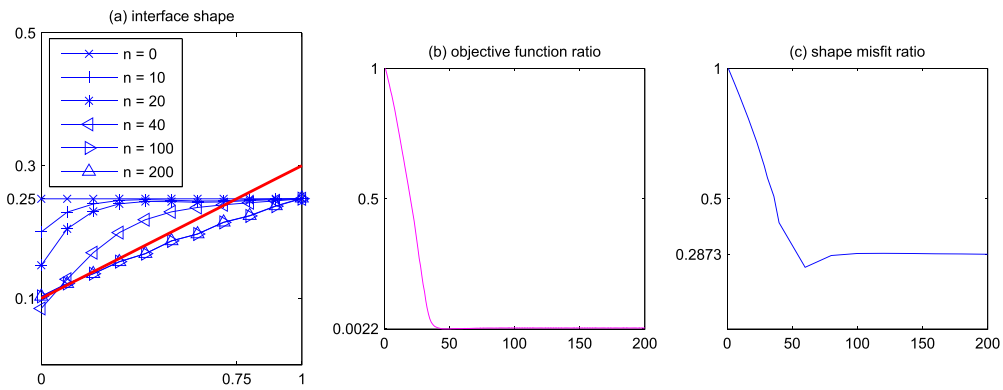


Figure 5. Iterations of breaking line $\Sigma^{(n)}$ with contact (a), objective ratio $\mathcal{J}^{(n)}/\mathcal{J}^{(0)}$ (b), and shape misfit ratio $R(n)$ (c).

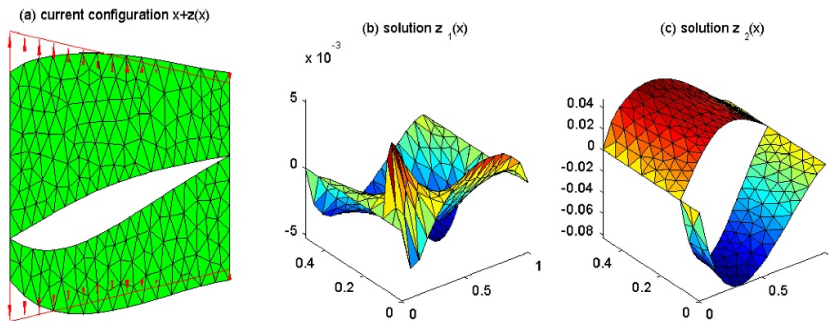


Figure 6. The true solution z_h without contact computed in current configuration (a) and componentwise (b), (c).

The selected iterations $n = 0, 10, 20, 40, 100, 200$ of $\Sigma^{(n)}$ according to (4.11) are presented in plot (a) together with the true Σ , which is marked with the thick solid line. In plot (b) of figure 5 we draw the ratio $\mathcal{J}^{(n)}/\mathcal{J}^{(0)}$ of the objective function versus $n \in [0, 200]$. The computed ratio attains as minimum 0,22%. In plot (c) the shape misfit ratio

$$R(n) := \frac{\|\Sigma^{(n)} - \Sigma\|}{\|\Sigma^{(0)} - \Sigma\|}, \quad \text{where } \|\Sigma^{(n)} - \Sigma\| := \|\psi^{(n)} - \psi\|_{C([0,1])} \quad (4.12)$$

is plotted, which attains as minimum 28,73%. We note that the computation is presented for the small penalty parameter $\varepsilon = 10^{-10}$, while larger values may cause some increase of the ratio curves after reaching the minimum.

From the simulation it can be observed in figure 5(a) that the left part of Σ without contact is recovered well, whereas the right part of interface being in contact (see figure 4(a)) is not approached during the iteration.

To remedy the hidden part, we apply the boundary force

$$g_1 \equiv 0, \quad g_2(x_1, 0.5) = (1 - 1.25x_1)\mu_L, \quad g_2(x_1, 0) = -g_2(x_1, 0.5), \quad (4.13)$$

which is more stretching than g in (4.3). Now the whole Σ is open as can be seen in figure 6.

The numerical result of the identification algorithm is depicted in figure 7.

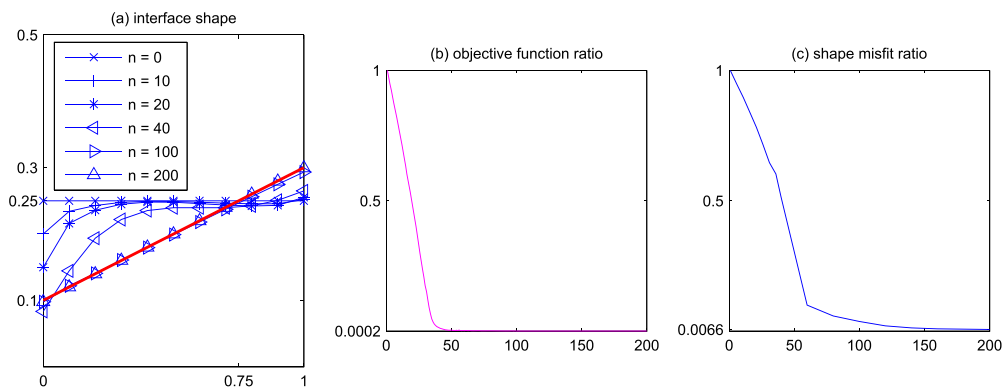


Figure 7. Iterations of breaking line $\Sigma^{(n)}$ without contact (a), objective ratio $\mathcal{J}^{(n)}/\mathcal{J}^{(0)}$ (b), and shape misfit ratio $R(n)$ (c).

Here plot (a) presents the selected iterations of $\Sigma^{(n)}$, plot (b) shows the objective ratio attaining as minimum 0,02%, and plot (c) demonstrates the shape misfit ratio $R(n)$ from (4.12), which decays to 0,66%. Now the whole Σ seen in figure 7 is recovered very accurate by algorithm 1.

5. Conclusion

The paper is a part of research on directional differentiability of shape control problems subjected to VIs and its applications to inverse problems in nonlinear fracture mechanics. In the previous work [32] we developed the general theory of shape differentiability for nonconvex problems, and we applied it to the contact problem for a cohesive energy, which is non-convex one. The new result is obtained for the surface energy, which is now convex one, but it was not considered before in the context of inverse identification problems. From the point of view of the theory of inverse and ill-posed problems, we have investigated how the key property of convexity affects identifiability of a shape being under unilateral contact conditions. On the basis of this contribution we conclude that the identification result is influenced not at first by convexity, rather contact conditions in the complementarity form or its penalty approximation.

From our numerical simulation tests we make a conclusion that the suggested algorithm of breaking-line identification is physically consistent with the setup of destructive physical analysis (DPA), where a defect is being opened. The DPA is widely used experimental technique to detect the failure of a specimen.

Data availability statement

No new data were created or analysed in this study.

Acknowledgment

The author acknowledges the financial support by the University of Graz.

ORCID iDVictor A Kovtunenکو  <https://orcid.org/0000-0001-5664-2625>**References**

- [1] Alekseev G V and Spivak Y E 2018 Theoretical analysis of the magnetic cloaking problem based on an optimization method *Differ. Equ.* **54** 1125–36
- [2] Alphonse A, Hintermüller M and Rautenberg C N 2022 Optimal control and directional differentiability for elliptic quasi-variational inequalities *Set-Valued Var. Anal.* **30** 873–922
- [3] Barenblatt G I 1959 The formation of equilibrium cracks during brittle fracture general ideas and hypotheses axially-symmetric cracks *J. Appl. Math. Mech.* **23** 622–36
- [4] Bonnet M and Cakoni F 2019 Analysis of topological derivative as a tool for qualitative identification *Inverse Problems* **35** 104007
- [5] Bredies K and Lorenz D A 2008 Linear convergence of iterative soft-thresholding *J. Fourier Anal. Appl.* **14** 813–37
- [6] Cakoni F and Kovtunenکو V A 2018 Topological optimality condition for the identification of the center of an inhomogeneity *Inverse Problems* **34** 035009
- [7] Casas E, Kunisch K and Tröltzsch F 2022 Optimal control of PDEs and FE-approximation *Handbook of Numerical Analysis* vol 23, ed E Trélat and E Zuazua (Amsterdam: North-Holland) pp 115–63
- [8] Chen L, Hassan H, Tallman T N, Huang S S and Smyl D 2022 Predicting strain and stress fields in self-sensing nanocomposites using deep learned electrical tomography *Smart Mater. Struct.* **31** 045024
- [9] Correa R and Seeger A 1985 Directional derivative of a minimax function *Nonlinear Anal. Theory Methods Appl.* **9** 834–62
- [10] Coulomb C A 1776 *Essai Sur une Application des Regles de Maximis et Minimis Quelques Problemes de Statique, Relatifs a l'Architecture* vol 7 (Paris: Memoires Acad Science)
- [11] Delfour M C and Zolésio J-P 2011 *Shape and Geometries: Metrics, Analysis, Differential Calculus and Optimization* (Philadelphia, PA: SIAM)
- [12] Ekeland I and Temam R 1976 *Convex Analysis and Variational Problems* (Amsterdam: North-Holland)
- [13] Francú J 1994 Weakly continuous operators. Applications to differential equations *Appl. Math.* **39** 45–56
- [14] Führ B, Schulz V and Welker K 2018 Shape optimization for interface identification with obstacle problems *Vietnam J. Math.* **46** 967–85
- [15] Furtsev A I, Itou H and Rudoy E M 2020 Modeling of bonded elastic structures by a variational method: Theoretical analysis and numerical simulation *Int. J. Solids Struct.* **182–183** 100–11
- [16] Ghilli D, Kunisch K and Kovtunenکو V A 2020 Inverse problem of breaking line identification by shape optimization *J. Inverse Ill-Posed Problems* **28** 119–35
- [17] González Granada J R and Kovtunenکو V A 2021 A shape derivative for optimal control of the nonlinear Brinkman–Forchheimer equation *J. Appl. Numer. Optim.* **3** 243–61
- [18] Griffith A A 1921 The phenomena of rupture and flow in solids *Phil. Trans. R. Soc. A* **221** 582–93
- [19] Gwinner J, Jadamba B, Khan A A and Raciti F 2021 *Uncertainty Quantification in Variational Inequalities* (Boca Raton, FL: Chapman and Hall/CRC)
- [20] Haslinger J, Kozubek T, Kunisch K and Peichl G 2003 Shape optimization and fictitious domain approach for solving free boundary problems of Bernoulli type *Comput. Optim. Appl.* **26** 231–51
- [21] Hauptmann A, Ikehata M, Itou H and Siltanen S 2019 Revealing cracks inside conductive bodies by electric surface measurements *Inverse Problems* **35** 025004
- [22] Heinemann C and Sturm K 2016 Shape optimization for a class of semilinear variational inequalities with applications to damage models *SIAM J. Math. Anal.* **48** 3579–617
- [23] Hintermüller M, Kovtunenکو V A and Kunisch K 2005 Generalized Newton methods for crack problems with nonpenetration condition *Numer. Methods Partial Differ. Equ.* **21** 586–610
- [24] Hintermüller M and Laurain A 2011 Optimal shape design subject to elliptic variational inequalities *SIAM J. Control Optim.* **49** 1015–47
- [25] Ito K and Kunisch K 2008 *Lagrange Multiplier Approach to Variational Problems and Applications* (Philadelphia, PA: SIAM)

- [26] Johnson K L, Kendall K and Roberts A D 1971 Surface energy and the contact of elastic solids *Phil. Trans. R. Soc. A* **324** 301–13
- [27] Khludnev A M and Kovtunenکو V A 2000 *Analysis of Cracks in Solids* (Boston, FL: WIT-Press)
- [28] Khludnev A M, Kovtunenکو V A and Tani A 2000 Evolution of a crack with kink and non-penetration *J. Math. Soc. Japan* **60** 1219–53
- [29] Kovtunenکو V A 2004 Numerical simulation of the non-linear crack problem with non-penetration *Math. Meth. Appl. Sci.* **27** 163–79
- [30] Kovtunenکو V A and Kunisch K 2007 Problem of crack perturbation based on level sets and velocities *Z. Angew. Math. Mech.* **87** 809–30
- [31] Kovtunenکو V A and Kunisch K 2014 High precision identification of an object: optimality-conditions-based concept of imaging *SIAM J. Control Optim.* **52** 773–96
- [32] Kovtunenکو V A and Kunisch K 2022 Shape derivative for penalty-constrained nonsmooth-nonconvex optimization: cohesive crack problem *J. Optim. Theory Appl.* **194** 597–635
- [33] Kovtunenکو V A and Ohtsuka K 2018 Shape differentiability of Lagrangians and application to Stokes problem *SIAM J. Control Optim.* **56** 3668–84
- [34] Laurain A and Sturm K 2016 Distributed shape derivative via averaged adjoint method and applications *ESAIM Math. Model. Numer.* **50** 1241–67
- [35] Lavrentiev M M, Avdeev A V, Lavrentiev M M Jr and Priimenکو V I 2003 *Inverse Problems of Mathematical Physics* (Leiden: VSP Publications)
- [36] Lazarev N P and Rudoy E M 2022 Optimal location of a finite set of rigid inclusions in contact problems for inhomogeneous two-dimensional bodies *J. Comput. Appl. Math.* **403** 113710
- [37] Marchuk G I, Agoshkov V I and Shutyaev V P 1996 *Adjoint Equations and Perturbation Algorithms in Nonlinear Problems* (Boca Raton, FL: CRC Press)
- [38] Meyer C, Rösch A and Tröltzsch F 2006 Optimal control of PDEs with regularized pointwise state constraints *Comput. Optim. Appl.* **33** 209–28
- [39] Popova E and Popov V L 2018 Note on the history of contact mechanics and friction: interplay of electrostatics, theory of gravitation and elasticity from Coulomb to Johnson-Kendall-Roberts theory of adhesion *Phys. Mesomech.* **21** 1–5
- [40] Rizzoni R, Dumont S, Lebon F and Sacco E 2014 Higher order model for soft and hard elastic interfaces *Int. J. Solids Struct.* **51** 4137–48
- [41] Shcherbakov V V 2022 Shape derivatives of energy and regularity of minimizers for shallow elastic shells with cohesive cracks *Nonlinear Anal. Real World Appl.* **65** 103505
- [42] Sofonea M and Migórski S 2017 *Variational–Hemivariational Inequalities With Applications* (Boca Raton, FL: Chapman and Hall/CRC)
- [43] Sokołowski J 1987 Sensitivity analysis of the Signorini variational inequality *Partial Differential Equations (Warsaw, 1984)* vol 19 (PWN Warsaw: Banach Center Publ) pp 287–99
- [44] Sokołowski J and Zolesio J-P 1992 *Introduction to Shape Optimization: Shape Sensitivity Analysis* (Berlin: Springer)
- [45] Tserpes K *et al* 2022 A review on failure theories and simulation models for adhesive joints *The J. Adhes.* **98** 1855–915
- [46] Zheltov Y P and Khristianovich S A 1955 On the mechanism of hydraulic fracturing in an oil-bearing bed *Izv. Akad. Nauk SSSR, Otd. Tech. Nauk* **5** 3–41